energies

MDPI

Article

Thermodynamic Analysis of Negative CO_2 Emission Power Plant Using Aspen Plus, Aspen Hysys, and Ebsilon Software

Paweł Ziółkowski [1], Paweł Madejski [2,*], Milad Amiri [1], Tomasz Kuś [2], Kamil Stasiak [1], Navaneethan Subramanian [2], Halina Pawlak-Kruczek [3], Janusz Badur [4], Łukasz Niedźwiecki [3] and Dariusz Mikielewicz [1]

[1] Faculty of Mechanical Engineering and Ship Technology, Institute of Energy, Gdańsk University of Technology, 80-233 Gdańsk, Poland; pawel.ziolkowski1@pg.edu.pl (P.Z.); milad.amiri@pg.edu.pl (M.A.); kamil.stasiak@pg.edu.pl (K.S.); dariusz.mikielewicz@pg.edu.pl (D.M.)
[2] Faculty of Mechanical Engineering, Department of Power Systems and Environmental Protection Facilities, AGH University of Science and Technology, 30-059 Kraków, Poland; kus@agh.edu.pl (T.K.); subraman@agh.edu.pl (N.S.)
[3] Department of Energy Conversion Engineering, Faculty of Mechanical and Power Engineering, Wroclaw University of Science and Technology, 50-370 Wrocław, Poland; halina.pawlak@pwr.edu.pl (H.P.-K.); lukasz.niedzwiecki@pwr.edu.pl (Ł.N.)
[4] Energy Conversion Department, Institute of Fluid Flow Machinery, Polish Academy of Sciences, 80-231 Gdańsk, Poland; jb@imp.gda.pl
* Correspondence: madejski@agh.edu.pl

Abstract: The article presents results of thermodynamic analysis using a zero-dimensional mathematical models of a negative CO_2 emission power plant. The developed cycle of a negative CO_2 emission power plant allows the production of electricity using gasified sewage sludge as a main fuel. The negative emission can be achieved by the use this type of fuel which is already a "zero-emissive" energy source. Together with carbon capture installation, there is a possibility to decrease CO_2 emission below the "zero" level. Developed models of a novel gas cycle which use selected codes allow the prediction of basic parameters of thermodynamic cycles such as output power, efficiency, combustion composition, exhaust temperature, etc. The paper presents results of thermodynamic analysis of two novel cycles, called PDF0 and PFD1, by using different thermodynamic codes. A comparison of results obtained by three different codes offered the chance to verify results because the experimental data are currently not available. The comparison of predictions between three different software in the literature is something new, according to studies made by authors. For gross efficiency (54.74%, 55.18%, and 52.00%), there is a similar relationship for turbine power output (155.9 kW, 157.19 kW, and 148.16 kW). Additionally, the chemical energy rate of the fuel is taken into account, which ultimately results in higher efficiencies for flue gases with increased steam production. A similar trend is assessed for increased CO_2 in the flue gas. The developed precise models are particularly important for a carbon capture and storage (CCS) energy system, where relatively new devices mutually cooperate and their thermodynamic parameters affect those devices. Proposed software employs extended a gas–steam turbine cycle to determine the effect of cycle into environment. First of all, it should be stated that there is a slight influence of the software used on the results obtained, but the basic tendencies are the same, which makes it possible to analyze various types of thermodynamic cycles. Secondly, the possibility of a negative CO_2 emission power plant and the positive environmental impact of the proposed solution has been demonstrated, which is also a novelty in the area of thermodynamic cycles.

Keywords: CCS; CO_2 negative power plant; Aspen Plus; Aspen Hysys; Ebsilon

Citation: Ziółkowski, P.; Madejski, P.; Amiri, M.; Kuś, T.; Stasiak, K.; Subramanian, N.; Pawlak-Kruczek, H.; Badur, J.; Niedźwiecki, Ł.; Mikielewicz, D. Thermodynamic Analysis of Negative CO_2 Emission Power Plant Using Aspen Plus, Aspen Hysys and Ebsilon Software. *Energies* **2021**, *14*, 6304. https://doi.org/10.3390/en14196304

Academic Editor: Francesco Nocera, Kyung Chun Kim, Marco Marengo

Received: 18 July 2021
Accepted: 24 September 2021
Published: 2 October 2021

1. Introduction

Decarbonization of the economy, specifically in energy generation sector, has been adopted as a world-wide policy with signing of the Paris Agreement by nearly 200 signatories, including most significant emitters [1]. Thus, an ambitious greenhouse gases reduction goals has been set, in order to prevent the average global temperature increasing more than 1.5 °C above the pre-industrial levels [1]. An extensive effort is needed to achieve such goal [2]. Fossil fuels contributed approximately 9.5 Gt of carbon emitted to the atmosphere on average per year, as highlighted by the global carbon budget for years 2009–2018 [3].

The United Nations Framework Convention on Climate Change (UNFCCC) has recognized carbon capture and storage (CCS) technologies as important means of achieving ambitious climate goals [4]. Parameters, such as efficiency, cost, and water, have been considered as extremely important factors, determining the success of CCS technologies [5]. The work completed on CCS so far has been focused on post-combustion CCS [6], its integration with power plants [7,8], and combustion with different oxygen concentrations, since dilution of CO_2 in flue gases influences capturing efficiency [9,10]. Furthermore, various emerging CCS technologies, such as membrane-based carbon capture and storage [11], pre-combustion CO_2 capture [12], or carbon sequestration in hydrates [13–15], are also subjects of intensive investigations.

1.1. Concept of Negative Emissions Power Plants Using Biomass

The concept of achieving negative emissions has recently caught some attention [16]. Using biomass, combined with CCS, to achieve negative CO_2 emissions, it is often described as bioenergy with carbon capture and storage (BECSS) [17]. Investigative efforts have been mainly focused on chemical looping combustion (CLC) of biomass [18], as well as co-combustion with coal [19]. Lyngfelt et al. [20] investigated possibilities of leakages of stored CO_2 and concluded that, due to expected time scales of such events, the contribution of such leakages to the atmospheric stock would be relatively small, reaching approximately 3 ppm of CO_2 [20]. The use of different types of biomass has been investigated, including the work of Niu et al. [21] on CLC of sewage sludge. Saari et al. [22] investigated BECSS, using CLC with oxygen uncoupling dedicated to large scale co-generation plant. The results have shown an extremely small efficiency penalty of 0.7%, along with CO_2 capturing efficiency being as high as 97% [22].

Nonetheless, other ways to practically apply BECSS are also being investigated. Lisbona et al. [17] evaluated synergy between biogas plant and a biomass power plant, with special attention to the CCS module. Proposed installation, utilizing 1.5 MW of biomass and 1.4 MW of biogas (power as chemical energy at the inlet), was able to generate 750 kW_{el} of electricity and generate 600 kW_{th} of heat, for its own needs [17]. Additionally, the installation was able to capture 1620 tons of CO_2 per year [17]. Buscheck and Upadhye [23] investigated hybrid approach, incorporating oxy-combustion and heat accumulation. Such a concept is important, not only from the point of view of negative CO_2 emissions, but also from the point of view of limiting the curtailment of energy generation using intermittent renewable energy sources [23], as flexibility is critical for power systems with high shares of intermittent renewable energy sources (solar, wind) [24–28]. Capron et al. [29] focused on the use of Allam Cycle for achieving carbon negative emissions. A comprehensive overview, as presented in that paper, suggested that CCS could be combined with growing seafood, its subsequent processing, and production of biofuels, resulting in simultaneous increase in productivity and decrease in the exploited surface of the oceans, thus increasing the overall areas dedicated to conservation of biodiversity [29].

However, practical application of BECSS solution could be costly. Cheng et al. [30] determined levelized costs of different BECSS solutions for the US state of Virginia reaching USD/ton$_{CO2}$ 82 (approx. EUR 70) for combustion of crop residues and USD/ton$_{CO2}$ 137

(approx. EUR 115) for combustion of woody residues. This is still much less than the current market value that could be assigned for a ton of avoided CO_2 emissions [31]. However, a study performed by Restrepo-Valencia and Walter [32] indicates that EUR/ton$_{CO2}$ 59 can be achieved for optimized BECSS using bagasse and the cost could be further decreased to EUR/ton$_{CO2}$ 48 for larger plants. This suggests that significant amount of work is needed to optimize BECSS in terms of CAPEX and OPEX. Such goal can be achieved by optimization of such systems, by comprehensive thermodynamic analysis.

1.2. Software for Zero-Dimensional Modelling

The zero-dimensional approach is mainly used for systems optimization. A limited amount of the obtained data makes it possible to conduct many optimizing calculations of the turbine parameters or entire complex system composed of many devices, such as compressors, expanders, heat exchangers, combustion chambers, reactors, fuel cells, pumps, or ejectors.

Literature on different software is very extensive; however, the most widely used ones are presented below, as follows:

- Aspen Plus is intended for a combined system, steam cycle, ORC cycle; operation under 50–110% nominal load [33];
- Aspen Hysys is intended for a combined system; operation under 50–110% nominal load and dynamic conditions [34];
- Ebsilon is designed for advanced steam block systems and combined systems, operation under variable conditions 40–120% of nominal load [35,36];
- Gate Cycle is designed for advanced combination systems, variable load operation 40–120% of nominal load [37];
- COM-GAS is intended for design level of combined systems with full analysis of a heat recovery steam generator, pulverized fuel, and fluidized bed boilers [38,39];
- DIAGAR is intended for design and diagnostic level of steam systems with full steam turbine analysis [40];
- IPSEpro is a process simulation tool, which is equation-oriented and has been used for power plant simulations, including modeling of chemical looping CCS systems [22];

The most important issue about software for thermodynamic cycles is that they have a high degree of certainty and confidence in the calculation results, which are only achieved by highly validated codes. This means that such codes, in addition to basic calculation algorithms, have extensive expert procedures for checking the results before they are passed on to the user. We selected three codes for detailed analysis of the considered case, namely Aspen Plus, Aspen Hysys, and Ebsilon. The following subsections provide a literature review on these codes.

1.3. Scope and Aim

The main objective of this paper is to analyze an innovative technology together with the proof of concept, confirming the possibility of the use of sewage sludge to produce electricity while having a positive impact on the environment. The synergy between the CCS plant and the proposed utilization of sewage sludge (which is considered a renewable energy source) enables the installation to achieve overall negative emissions of CO_2 (nCO2PP). Proposed processes of utilization (PFD0—Sections 2 and 3; PFD1—Sections 4 and 5), called nCO2PP (negative CO_2 Power Plant), ensures reaching of scientific objectives related to three essential theoretical elements, namely: (1) a system that processes sewage sludge into syngas; (2) a system that burns the resulting fuel in pure oxygen in a dedicated wet combustion chamber; and (3) a system of a unique turbine cooperating with a spray ejector condenser with carbon dioxide capture.

The second aim of the article is to compare the results obtained in three computing codes, namely Aspen Plus, Aspen HYSYS, and Ebsilon, based on the assumption presented in next section, and subsequently pointing out the differences and identifying the

reasons for them. Section 2 examines the original simple system consisting of an arrangement of equipment such as compressors, expanders, heat exchanger, combustion chamber, pump, and generator to generate electrical energy. A schematic of the cycle can be found in Figure 1, while Figure 2 presents the model in Aspen Hysys, Figure 3 in Aspen plus, and Figure 4 in Ebsilon. Section 3 presents the following subsections as follows: (1) thermodynamic parameters and mass flow rates in nodal points; (2) the output and efficiencies of power; and (3) the effect of NOx production on combustion chamber temperature. In Section 4, this system is extended to include a spray ejector condenser, where diagrams of power output, efficiency, and chemical energy flow delivered to the combustion chamber are prepared for clarity of results. In Section 5, it is shown that this gas-fired power plant, after the use of gasification fuel (the composition of mixture 1 is given as an example), is CO_2-negative. The last section summarizes the work carried out and draws conclusions.

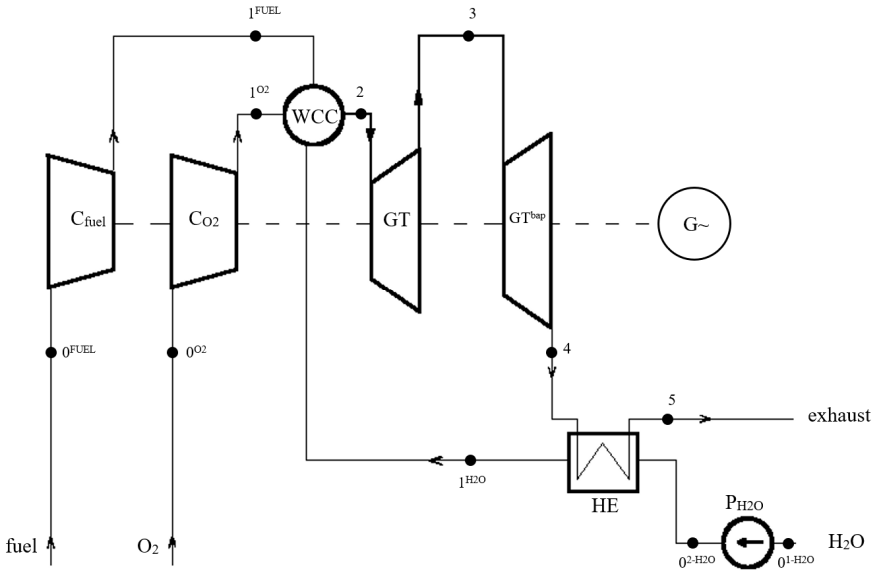

Figure 1. Process flow diagram of a gas mixture cycle PFD0—a steam-gas turbine system (0FUEL, $0O_2$, 01-H_2O, 02-H_2O, 1FUEL, $1O_2$, $1H_2O$, 2, 3, 4, 5—cycle nodal points).

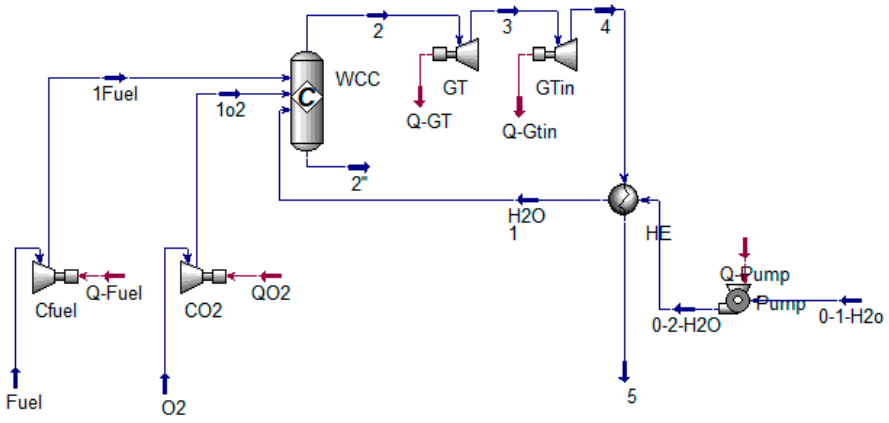

Figure 2. Simulation of PFD0 by Aspen Hysys (0FUEL, $0O_2$, 01-H_2O, 02-H_2O, 1FUEL, $1O_2$, $1H_2O$, 2, 3, 4, 5—cycle nodal points).

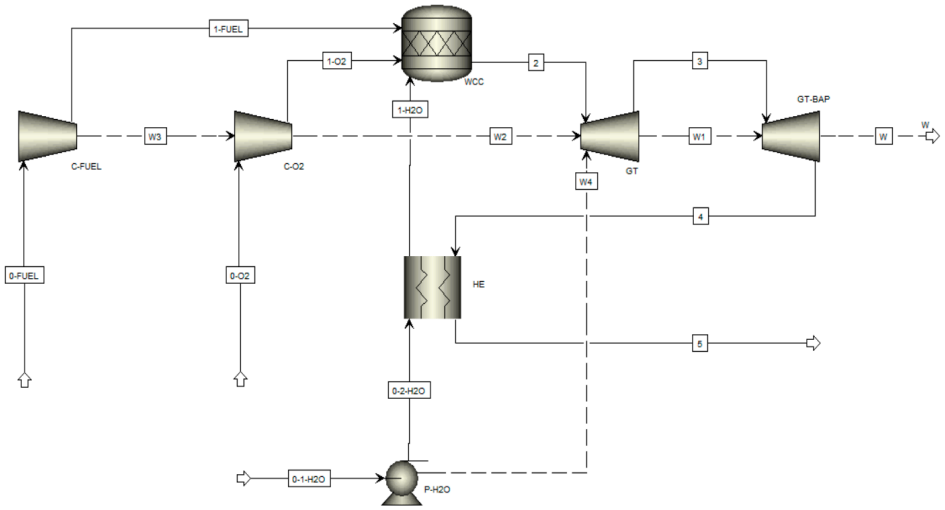

Figure 3. Simulation of PFD0 by Aspen Plus (0FUEL, $0O_2$, 01-H_2O, 02-H_2O, 1FUEL, $1O_2$, $1H_2O$, 2, 3, 4, 5—cycle nodal points).

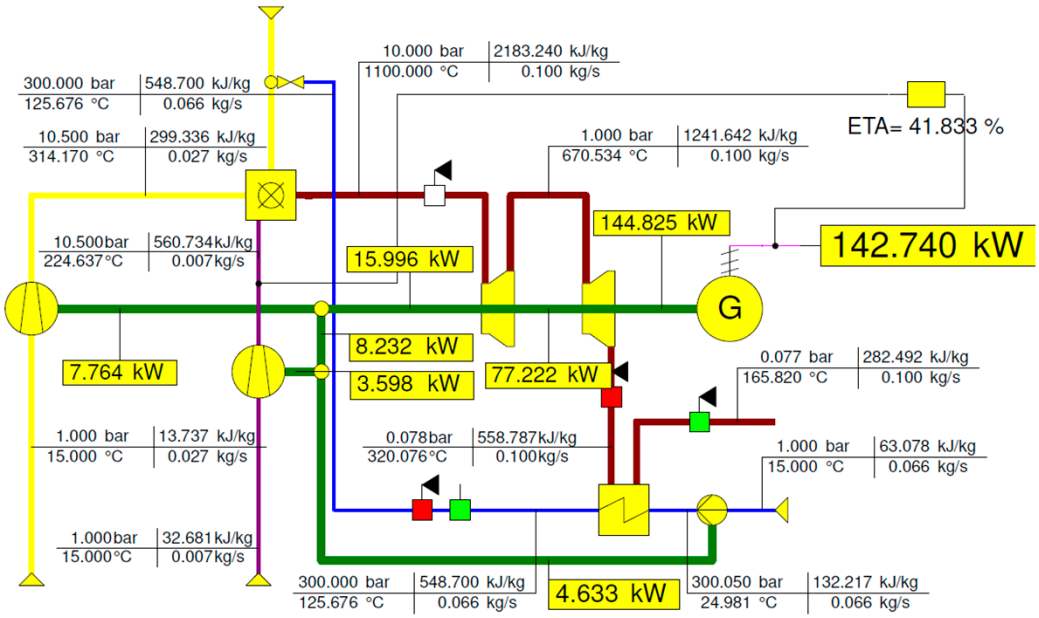

Figure 4. Simulation of PFD0 by Ebsilon (0FUEL, $0O_2$, 01-H_2O, 02-H_2O, 1FUEL, $1O_2$, $1H_2O$, 2, 3, 4, 5—cycle nodal points).

2. Thermodynamic Cycle Considered in Three Software

2.1. Modeling and Simulation of Thermodynamic Cycles

The use of thermodynamic simulation software can strongly support designing, monitoring, and optimizing CCUS processes as the new solutions for existing and planned to build power plants.

Different perspectives of modeling has been created by Aspen Plus, such as steam power plant [41], predicting emissions of NO and N_2O from coal combustion [42], catalytic coal gasification infixed beds [43], biomass gasification in fluidized bed reactor [44], and in combined heat and power (CHP) biomass bubbling fluidized bed gasification unit coupled with an internal combustion engine (ICE) [45]. Ebsilon®Professional is a simulation software designed for performing simulations of processes in thermodynamic cycles, as well as steady-state and quasi dynamic simulations [46–49]. The Ebsilon library has an extensive number of components, useful for efficient calculations [49]. By placing the com-

ponents in the system, a system of equations is generated based on mass and energy balance depending upon the component, which is solved by the Gauss–Seidel method. The iteration ends when the convergence criterion of 10-9 is reached for pressure, flow, and enthalpy variables [50]. Aspen HYSYS is defined as an industry-leading process modeling tool for conceptual study, strategic planning, management of asset, maximization and operational testing for gas processing, petroleum refining, oil and gas production, and air separation industries. Although HYSYS is mainly useful for oil and gas process industry, it is developed for various industries as follows [51]: ethanol plant; petroleum industry; heavy chemical industry; natural gas process plant; petrochemical industry; synthesis gas production; acid gas sweetening with DEA (Diethanolamine); biodiesel plant, etc. A comparison of units in Aspen Plus, Aspen HYSYS, and EBSILON is presented in Table 1.

Table 1. Comparison of units in Aspen Plus, Aspen HYSYS, and EBSILON.

Unit Operation	Aspen Plus	Aspen HYSYS	EBSILON
Stream mixing	Mixer	Mixer	Simple mixer
Component splitter	Sep, Sep2	Component Splitter	Simple splitter
Decanter	Decanter	3-Phase Separator	Selective splitter
Piping	Pipe, Pipeline	Pipe Segment, Compressible Gas Pipe	Pipe
Valves and fittings	Valve	Valve, Tee, Relief Valve	Valve
Equilibrium reactor	REquil	Equilibrium Reactor	Combustion chamber
Gibbs reactor	RGibbs	Gibbs Reactor	Gibbs reactor
Heat exchanger	HeatX, HxFlux, Hetran, HTRI-Xist	Heat Exchanger	Heat exchanger
Compressor	Compr, MCompr	Compressor	Compressor
Turbine	Compr, MCompr	Expander	Gas expander
Pump	Pump	Pump	Pump

Differences and similarities of thermodynamic parameters for the three used software including Aspen Hysys, Plus, and Ebsilon are indicated in Table 2. Crucial parameters for thermodynamic is its efficiency, which depend from many issues, but one of the important is model of fluid. The net system efficiency of the system was calculated according to the formula:

$$\eta_{net} = \frac{N_t - N_{C-fuel} - N_{C-O_2} - N_{P-H_2O} - N_{CCU} - N_{p-SEC}}{\dot{Q}_{CC}} \quad (1)$$

where:

N_t—combined turbine power on the shaft in [kW],

N_{C-fuel}—power for fuel compressor in [kW],

N_{C-O_2}—power for oxygen compressor in [kW],

N_{P-H_2O}—power for water pump PH2O in [kW],

N_{P-SEC}—power for water pump PSEC supplying SEC in [kW],

N_{CCU}—combined power for CO_2 capture unit compressors [kW],

$\dot{Q}_{CC}$—chemical energy rate of combustion in [kW].

Important is also power for own needs as a sum:

$$N_{CP} = N_{C-fuel} + N_{C-O2} + N_{P-H2O} + N_{P-SEC} + N_{CCU} \quad (2)$$

According this equation, the powers depend from thermodynamic model of fluid which is possible to describe the real gas equation in a more precise form, which takes the form of the Peng–Robinson gas model:

$$p = \frac{\tilde{R}T}{v_M - b} - \frac{a\alpha_m}{v_M^2 + 2bv_M - b^2}, \tag{3}$$

where: $\tilde{R}$—universal gas constant, v_M—molar volume and

$$a = \frac{0.4572\tilde{R}^2 T_{cr(m)}^2}{p_{cr(m)}} \tag{4}$$

where: $p_{cr(m)}$—critical pressure, $T_{cr(m)}$—critical temperature. Another constant is:

$$b = \frac{0.0778\tilde{R}T_{cr(m)}}{p_{cr(m)}} \tag{5}$$

and the last constant from the Formula (3) is expressed as:

$$\alpha_m = (1 + \xi_m(1 - T_{r(m)}^{0.5}))^2 \tag{6}$$

assuming that the reduced temperature $T_{r(m)}$ expresses the ratio:

$$T_{r(m)} = \frac{T}{T_{cr(m)}} \tag{7}$$

and

$$\xi_m = 0.37464 + 1.54226\omega_m - 0.26992\omega_m^2 \tag{8}$$

where ω_m is the material constant expressing the molecular non-sphericity (centrality) of the particles. For example, for noble gases such as argon, krypton, neon, and xenon $\omega_m = 0$. It should be also mentioned that ω_m is determined for $T_{r(m)} = 0.7$ and can be determined by the relationship:

$$\omega_m = -\log_{10}\left(p_{r(m)}^{sat}\right) - 1 \tag{9}$$

where $p_{r(m)}^{sat}$ is the reduced evaporation pressure expressed as the relationship:

$$p_{r(m)}^{sat} = \frac{p_{sat(m)}}{p_{cr(m)}} \tag{10}$$

where $p_{sat(m)}$ is the saturation pressure (evaporation) for $T_{r(m)} = 0.7$.

Although Peng-Robinson as a thermodynamic model is used for both Aspen Hysys and Plus, thermodynamic tables for steam and Peng-Robinson for another working fluid are used in Ebsilon.

Table 2. Differences and similarities for calculations.

Parameter	Symbol	Unit	
Thermodynamic model	Peng-Robinson	-	Thermodynamics tables for steam and Peng-Robinson for another working fluid
Net efficiency	*η_net*	-	$\frac{N_t - N_{C-fuel} - N_{C-O_2} - N_{P-H_2O} - N_{CCU} - N_{p-SEC}}{\dot{Q}_{CC}}$
Gross efficiency	η_g	-	$\eta_g = \frac{N_t}{\dot{Q}_{CC}}$
NOx production	NO and NO_2	-	Without NOx production calculation in Ebsilon software
Chemical energy rate	$\dot{Q}_{CC}$	kW	$\dot{Q}_{CC} = \dot{m}_{fuel} LHV$
Reactions	combustion	-	Defined and could be modified

It should be underscored that the specific enthalpy of the fluid $h = h(p;T;Y_{(k)})$ is determined at the characteristic points by the thermodynamic table and depends on thermodynamic parameters, such as temperature T, pressure p, and specific components within the mixture of air and exhaust gases $Y_{(k)}$; $k = N_2,\ldots, Ar$ [52,53]. Another difference can be tangible in NO_x production so that Aspen Hysys and Plus calculate NO_x production including NO and NO_2, whilst it is not estimated in Ebsilon. In addition, reactions used in wet combustion chamber need to be defined in properties tab (Reaction's part) in Aspen Hysys. As it can be vividly seen, the method of calculating net efficiency, gross efficiency, and chemical energy rate is the same for three used software.

2.2. Thermodynamic Cycle

The thermodynamic cycle of the gas–steam turbine system is represented in Figure 1. The gas–steam turbine system consists of two gas–steam expanders, i.e., the gas–steam turbine (GT) part and the low-pressure gas–steam turbine below ambient pressure (GT_{bap}) with power generators (G~), the fuel compressor (C_{fuel}), the oxygen compressor (C_{O2}), the water pump (P_{H2O}), the heat exchanger (HE) for regenerative water heating, and the wet combustion chamber (WCC). The working fluid in the cycle is the gas–steam—a mixture of water vapor (H_2O) and carbon dioxide (CO_2). As observed in Figure 1, after increasing the pressure of selected fuel (methane and mixture 1) and O_2 in their related compressor, they are fed to a wet combustion chamber. Wet combustion chamber combusts selected fuels in the presence of oxygen O_2 to produce hot steam and carbon dioxide. Using the recycled water leads hot steam and carbon dioxide to cool within the wet combustion chamber to the desired temperature of a gas turbine. GT and GT_{bap} are used to decrease high-pressure (10 bar) working fluid (water vapor and carbon dioxide) to below ambient pressure (0.078 bar). A heat exchanger is not only simulated to achieve the cooled steam but also increases the temperature of water.

2.3. Assumptions for Cycle Modeling

Assumptions for the thermodynamic cycle, internal efficiency, and mechanical efficiency are illustrated in Tables 3–5. It can be noticed that the temperature of exhaust gas after WCC (before GT) is 1100 °C in Aspen Hysys and Plus and Ebsilon for (Ebsilon t_2 = const), while for Ebsilon t_2 = var is 1073 °C for methane and 1091 °C for mixture 1, respectively. These temperatures (namely 1100 °C in Aspen Plus and Aspen Hysys, and 1091 °C and 1073 °C) in front of the turbine were achieved by assuming a constant temperature of water feeding the combustion chamber, namely t_1H_2O = const = 125.1 °C. In addition, when the exhaust temperature after WCC is constant (t_2 = 1100 °C), water temperature before the combustion chamber is variable, respectively, 149.02 °C in Ebsilon with mixture 1, 131.84 °C in Ebsilon with methane, and 125.1 °C for both Aspen Hysys and Plus. Heat efficiency of the combustion chamber in Aspen Plus and Aspen Hysys is 99.9%. The rest of the assumptions for the three used software is the same.

Table 3. Assumptions for the thermodynamic cycle calculation using Aspen HYSYS, Aspen Plus, and Ebsilon.

Parameters	Symbol	Unit	Value
Mass flow of exhaust gas at the outlet from combustion chamber WCC	m_2	g/s	100
Air-fuel ratio in WCC	λ	-	1 (stoichiometric)
Pressure before GT	p_2	bar	10
Pressure after GT	p_3	bar	1
Pressure after GT_{bap}	p_4	bar	0.078
Water pressure to WCC	$p_{1\text{-}H2O}$	bar	300
Temperature exhaust after WCC (before GT)	t_2	°C	1100 (1100 and variable in Ebsilon)

Initial water temperature (before PH2O pump)		$t_{0\text{-}1\text{-}H2O}$	°C	15
Initial fuel temperature		t_{fuel}	°C	15
Initial oxygen temperature		t_{O2}	°C	15
Initial fuel pressure (before Cfuel compressor)		$p_{0\text{-}fuel}$	bar	1
Initial oxygen pressure (before CO2 compressor)		$p_{0\text{-}O2}$	bar	1
Fuel to WCC pressure loss factor		δ_{fuel}	-	0.05
Oxygen to WCC pressure loss factor		δ_{O2}	-	0.05
Oxygen purity			%	100
Fuel mass flow	methane	$\dot{m}_{fuel}$	g/s	6.72
	Mixture—syngas	$\dot{m}_{fuel}$	g/s	18.00
Temperature exhaust after WCC (before GT)	Variable temperature in point 1H2O (118.45; 131.84 and 125.1 °C)	$t_2 = const$	°C	1100
	Constant temperature in point 1H2O (125.1 °C)	$t_2 = var$	°C	1100 1073 for mixture, 1091 for methane in Ebsilon
CO_2 fraction from combustion of methane	Methane	$X_{co_2} = const$	mol%	8.47
	Mixture	$X_{CO_2} = var$	mol%	11.75 11.73 in Ebsilon
Water temperature before combustion chamber	Variable temperature exhaust after WCC	$t_{1\,H_2O} = const$	°C	125.1
	Constant temperature exhaust after WCC	$t_{1\,H_2O} = var$	°C	149.02 for mixture and 131.84 for methane in Ebsilon

Table 4. Assumed internal efficiency (adiabatic for Hysys and isentropic for Aspen Plus and Ebsilon).

Internal Efficiency	Symbol	Unit	Value
Turbine GT	η_{iGT}	-	0.89
Turbine GT_{bap}	$\eta_{iGT\text{-}bap}$	-	0.89
Fuel compressor C_{fuel}	$\eta_{iC\text{-}fuel}$	-	0.87
Oxygen compressor C_{O2}	$\eta_{iC\text{-}O2}$	-	0.87
Water pump P_{H2O}	$\eta_{iP\text{-}H2O}$	-	0.43

Table 5. Assumed mechanical efficiency—for Aspen Hysys it is impossible to change value.

Internal Efficiency	Symbol	Unit	Aspen HYSYS	Aspen Plus/EBSILON
Turbine GT	η_{mGT}	-	1	0.99
Turbine GT_{bap}	$\eta_{mGT\text{-}bap}$	-	1	0.99
Fuel compressor C_{fuel}	$\eta_{mC\text{-}fuel}$	-	1	0.99
Oxygen compressor C_{O2}	$\eta_{mC\text{-}O2}$	-	1	0.99
Water pump P_{H2O}	$\eta_{mP\text{-}H2O}$	-	1	0.99

2.4. Fuels

Syngas fuels produced from gasification are expected to be of different compositions, mainly due to inherent variability of sewage sludge composition, as reported by Werle and Wilk [54]. Therefore, two types of fuel were selected for the analysis, and compositions are presented in Figure 5. The first one is the syngas mixture which contains CO (9.09%$_{mol}$); CO_2 (25.61%$_{mol}$); CH_4 (13.64%$_{mol}$); C_3H_8 (3.39%$_{mol}$); H_2 (45.16%$_{mol}$); and NH_3 (3.10%$_{mol}$). However, the mass fractions of species for Aspen Plus and Aspen Hysys was introduced as data, namely CO (13.31%$_{mass}$); CO_2 (59.31%$_{mass}$); CH_4 (11.46%$_{mass}$); C_3H_8 (8.03%$_{mass}$); H_2 (5.10%$_{mass}$); and NH_3 (2.79%$_{mass}$). Selected compositions of the producer gas are well within the ranges of values are reported by Achweizer et al. [55] or Akkache et

al. [56]. Methane fuel is added for comparison purposes. The compositions of selected fuels, including methane and mixture (syngas), are shown in Figure 5.

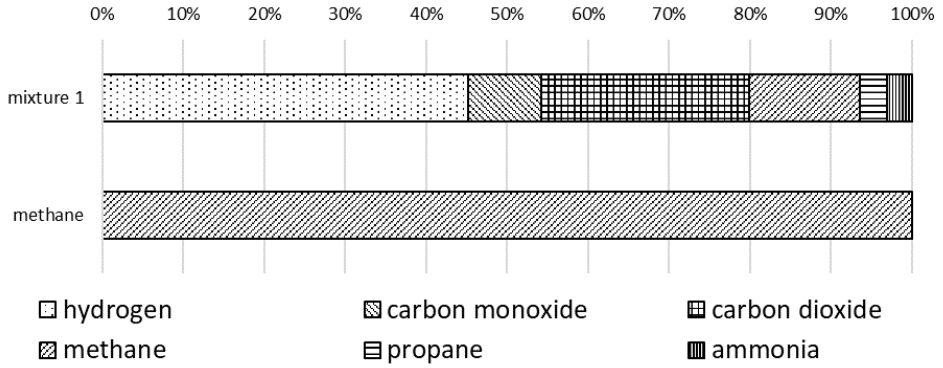

Figure 5. Fuel compositions for the analysed cycle.

The values of LHV for mixture 1 and methane at 15 °C and 1 atm are presented in Table 6. It is noteworthy that Ebsilon uses empirical formulae based on elementary analysis, whereas LHV used for both Aspen Hysys and Plus are the same. Syngas is produced by gasifying sewage sludge.

Table 6. LHV based on ISO 6976:1995(E) for gas mixtures, value at 15 °C and 1 atm derived from Aspen and Ebsilon.

Software	LHV, MJ/kg	
	Syngas—Mixture	Methane
Aspen HYSYS and Aspen PLUS	17.079	50.035
Ebsilon	17.081	50.015

3. Results and Comparison

The most important nodal point results are presented in Section 3.1, while Section 3.2 refers to the efficiency results and Section 3.3 deals with the combustion of ammonia to various nitrogen compounds.

3.1. Nodal Points

Cycle nodal points for mixture (syngas) and methane are depicted in Tables 7 and 8, respectively. Having studied the data from Table 7, it can be considered that mass flow of mixture (syngas), O_2, and H_2O are 18 (g/s), 23.19 (g/s), and 58.80 (g/s) in Aspen Hysys and Plus, whilst these values in Ebsilon are 18 (g/s), 22.84 (g/s), and 59.164 (g/s), respectively. It is noticeable that simulation in Ebsilon was performed for two values of t_2 (temperature after WCC), as mentioned in Table 3. The temperature after compressor of fuel (syngas) is 255.6 °C, 253.33 °C, and 252.38 °C and after compressor of O_2 is 314.8 °C, 315.08 °C, and 314.17 °C in Aspen Hysys, Plus, and Ebsilon, respectively. Other differences can be observed in temperature before and after the heat exchanger. More accurately, temperature before heat exchanger is 25.11 °C for both simulation in Apen Hysys and Plus, whereas its value is 24.98 °C in Ebsilon. These temperatures are obtained by increasing the pressure in the pump.

As the same way, the temperature after heat exchanger is 125.11 °C was the same for both simulations in Apen Hysys and Plus, while it is 125.11 °C and 149.02 °C for mixture 1, 125.11 °C and 131.84 °C for methane when t_2 = var and t_2 = const in Ebsilon, respectively. In addition, CO_2, H_2O, and NO (N_2 in Ebsilon) result from combustion in a wet combustion chamber. As seen in Table 7, mole fraction of CO_2 is 11.75 and 11.73 in Aspen Hysys, Plus, and Ebsilon, respectively. Moreover, mole fraction of H_2O is 87.63 and 87.98 for mentioned software, respectively. The most important difference in arising composition is in

the type of NO_x, so that there is NO (0.62) in Aspen Hysys and Plus, whereas N_2 (0.32) is created in Ebsilon. Although it is assumed that the temperature after wet combustion chamber is 1100 °C for Aspen Hysys, Plus, and Ebsilon, a different temperature (1073 °C) after WCC was simulated in Ebsilon. Results show that the maximum temperature of exhaust gases after the heat exchanger results from simulation of Aspen Plus and its value is 183.58 °C whereas the minimum one (147.3 °C) belongs to the simulation using Ebsilon (t_2 = const).

As it can be observed that the difference in temperature (324.7 °C in Hysys, 323.64 °C in Plus, and 324.82 °C in Ebsilon) before heat exchanger for gas–steam is less than 0.4%, the type of heat exchanger plays an indispensable role in regard to the value of cooled gas–steam (exhaust gases). In addition, pressure drop of heat exchanger is zero in Aspen Hysys and Plus, but a pressure drop is not constant in Ebsilon (pressure differences between point 4 and 5). Moreover, decreasing the temperature after wet combustion chamber leads to increasing the temperature of cooled gas–steam (t_5), so that approximately a 12% increase in temperature of steam after heat exchanger results from decreasing the temperature after WCC from 1100 to 1073 °C.

Cycle nodal points for methane are indicated in Table 8. Mass flow of fuel, O_2, and H_2O are the same for used software and its value is 6.72 (g/s), 26.80 (g/s), and 66.48 (g/s), respectively. Although the temperature of water that was fed to WCC is 125.11 °C, this value indicates for simulation various temperature in combustion chamber (t_2 = 1091 °C) in Ebsilon and (t_2 = 1100 °C) in Aspen Plus and Aspen Hysys. To obtain the same temperature in combustion chamber in simulation using a Ebsilon, we need to increase temperature to 131.84 °C. Moreover, a decrease (0.82%) in the temperature of exhaust gases after WCC from 1100 °C to 1091 °C results in an increase (3.6%) in temperature of cooled gas–steam after heat exchanger from 155.65 °C to 161.47 °C in Ebsilon.

As a result, changing the type of fuels leads to a change in the compositions of exhaust gases and temperature after a heat exchanger. For example, approximately 88% and 92% mole fraction of H_2O result from mixture 1 (syngas) and methane, respectively. Furthermore, using a mixture of gases as a fuel and methane result in creating approximately 12% and 8% mole fraction of CO_2. Moreover, the average temperature (among three software) after the heat exchanger is 169.3 °C for mixture and 160 °C for methane.

Table 7. Cycle nodal points on basis of syngas—mixture of gases as a fuel.

Parameter	Case	Unit	Value										
Node designation	**-**	**-**	**0 Fuel**	**1 Fuel**	**0^{O2}**	**1^{O2}**	**$0^{1\text{-}H2O}$**	**$0^{2\text{-}H2O}$**	**1^{H2O}**	**2**	**3**	**4**	**5**
Mass flow $\dot{m}$	Aspen Hysys Aspen Plus Ebsilon t_2 = var Ebsilon t_2 = const	g/s	18.0	18.0	23.2 22.4	23.2 22.4	58.8 59.6	58.8 59.6	58.8 59.6	100	100	100	100
O_2 fraction (X_{O_2})	Aspen Hysys Aspen Plus Ebsilon t_2 = var Ebsilon t_2 = const	mol%	- - - -	- - - -	100	100	- - - -	- - - -	- - - -	0.00	0.00	0.00	0.00
CO_2 fraction (X_{CO_2})	Aspen Hysys Aspen Plus Ebsilon t_2 = var Ebsilon t_2 = const	mol%	- - - -	- - - -	- - - -	- - - -	- - - -	- - - -	- - - -	11.75 11.73	11.75 11.73	11.75 11.73	11.75 11.73
H_2O fraction	Aspen Hysys Aspen Plus	mol%	- -	- -	- -	- -	100	100	100	87.63	87.63	87.63	87.63

(X_{H_2O})	Ebsilon t_2 = var		-	-	-	-							
	Ebsilon t_2 = const		-	-	-	-				87.96	87.96	87.96	87.96
	Aspen Hysys		-	-	-	-	-	-	-				
	Aspen Plus	mol%	-	-	-	-	-	-	-	0.62	0.62	0.62	0.62
NO fraction (N_2 in Ebsilon) (X_{NO})	Ebsilon t_2 = var		-	-	-	-	-	-	-				
	Ebsilon t_2 = const		-	-	-	-	-	-	-	0.31	0.31	0.31	0.31
	Aspen Hysys			255.6		314.8					672.5	324.7	178.6
	Aspen Plus	°C		253.33	15	315.08		25.11	125.11	1100	672.51	323.64	183.58
Temperature (t)	Ebsilon t_2 = const		15	252.38		314.17	15		149.02		673.58	324.86	147.3
	Ebsilon t_2 = var							24.98	125.11	1073	652.98	310.38	167.64
	Aspen Hysys												
Pressure (p)	Aspen Plus	bar	1	10.5	1	10.5	1	300	300	10	1	0.078	0.078
	Ebsilon t_2 = var												0.077
	Ebsilon t_2 = const												

Table 8. Cycle nodal points on basis of methane.

	Symbol	Unit	Value										
Node designation	**-**	**-**	**0 Fuel**	**1 Fuel**	**0^{O2}**	**1^{O2}**	**$0^{1\text{-}H2O}$**	**$0^{2\text{-}H2O}$**	**1^{H2O}**	**2**	**3**	**4**	**5**
Mass flow ($\dot{m}$)	Aspen Hysys												
	Aspen Plus	g/s	6.72	6.72	26.80	26.80	66.48	66.48	66.48	100	100	100	100
	Ebsilon t_2 = var												
	Ebsilon t_2 = const												
O_2 fraction (X_{O_2})	Aspen Hysys												
	Aspen Plus	mol%	-	-	100	100	-	-	-	0.00	0.00	0.00	0.00
	Ebsilon t_2 = var												
	Ebsilon t_2 = const												
CO_2 fraction (X_{CO_2})	Aspen Hysys												
	Aspen Plus	mol%	-	-	-	-	-	-	-	8.47	8.47	8.47	8.47
	Ebsilon t_2 = var												
	Ebsilon t_2 = const												
H_2O fraction (X_{H_2O})	Aspen Hysys												
	Aspen Plus	mol%	-	-	-	-					91.53	91.53	91.53
	Ebsilon t_2 = var						100	100	100	91.53			
	Ebsilon t_2 = const												
	Aspen Hysys					314.8					667.3	318.4	158.6
Temperature (t)	Aspen Plus	°C	15	225.39	15	315.08	15	25.11	125.11	1100	669.51	318.99	165.82
	Ebsilon t_2 = const			224.63		314.17		24.98	131.84		670.49	320.01	155.65

	Ebsilon t_2 = var								125.11	1091	663.9	315.35	161.47
Pressure (p)	Aspen Hysys	bar	1	10.5	1	10.5	1	300	300	10	1	0.078	0.078
	Aspen Plus												
	Ebsilon t_2 = var												
	Ebsilon t_2 = const												0.077

3.2. Efficiency and Summarized Effects

Summarized results for two fuels (mixture 1 and methane) in three used software including Aspen Hysys, Plus, and Ebsilon are illustrated in Table 9. The mass flow rate after WCC is 100 g/s for the three mentioned software. The gross power of turbines for mixture is 154.37 kW, 154.20 kW, 154.72 kW (t_2 = const), and 151.36 kW (t_2 = var) in Aspen Hysys, Plus, and Ebsilon, respectively. It can be observed that less than a 0.34% difference was obtained among three software, when t_2 is 1073 °C or 1100 °C. On the other hand, for methane, these values are 161.42 kW, 160.72 kW, 160.89 kW (t_2 = const), and 159.76 kW (t_2 = var) for the mentioned software, respectively. The results show that, at the same assumption, changing the type of fuels from mixture 1 to methane leads the gross power output of turbines to increase approximately by 4% in Aspen Hysys, Plus and Ebsilon (t_2 = const) and approximately by 5% in Ebsilon (t_2 = var).

According to calculation of chemical energy rate of combustion Q_{cc} mentioned in Tables 2 and 9, this value in used software is approximately 307 kW and 336 kW for mixture 1 and methane, respectively. The results represent that the net efficiency of the system is 44%, 43.8%, 44.16%, and 43.07% for mixture 1 in Aspen Hysys, Plus, Ebsilon (including t_2 = const and t_2 = variable), respectively. These values are 43.32%, 43.05%, 43.12%, and 42.8% for methane for the mentioned software, respectively. It can be found from the results of Aspen Hysys, Plus, and Ebsilon (t_2 = const) that, at the same assumption, changing fuels from methane to mixture results in rising the net efficiency of system from 1.5 to 2.4%.

The main source of the difference in the results obtained in Sections 3.1 and 3.2 is the fact that the specific heat was determined differently. This becomes apparent in the temperature results after pumps, compressors, and expanders.

Table 9. Effect of different fuels.

Parameter	Symbol	Unit	Mixture 1 (Syngas)	Methane
Temperature at the WCC outlet	t_2 = var	°C	1073	1091
	t_2 = const	°C	1100	1100
Fuel mass flow ($\dot{m}_{1-fuel}$)	Aspen Hysys Aspen Plus Ebsilon t_2 = var Ebsilon t_2 = const	g/s	18.00	6.72
Oxygen mass flow ($\dot{m}_{1-O2}$)	Aspen Hysys	g/s	23.2	26.8
	Aspen Plus Ebsilon t_2 = var		22.4	
	Ebsilon t_2 = const			
Water mass flow ($\dot{m}_{1-H2O}$)	Aspen Hysys	g/s	58.8	66.48
	Aspen Plus Ebsilon t_2 = var		59.6	
	Ebsilon t_2 = const			
Exhaust temperaturę after HE (t_5)	Aspen Hysys	°C	178.60	161.10
	Aspen Plus		183.58	165.82
	Ebsilon t_2 = var		167.64	161.47

	Ebsilon t_2 = const		147.3	155.65
Turbine power GT (N_{GT})	Aspen Hysys	kW	88.73	92.93
	Aspen Plus		89.30	93.20
	Ebsilon t_2 = var		87.67	92.65
	Ebsilon t_2 = const		89.53	93.26
Turbine power GT^{bap} (N_{GT-bap})	Aspen Hysys	kW	65.64	68.49
	Aspen Plus		64.9	67.52
	Ebsilon t_2 = var		63.69	67.11
	Ebsilon t_2 = const		65.20	67.63
Combined turbines gross power (N_t)	Aspen Hysys	kW	154.37	161.42
	Aspen Plus		154.20	160.72
	Ebsilon t_2 = var		151.36	159.76
	Ebsilon t_2 = const		154.72	160.89
Power for own needs (N_{cp})	Aspen Hysys	kW	19.12	15.75
	Aspen Plus		19.30	16
	Ebsilon t_2 = var		18.94	15.954
	Ebsilon t_2 = const			15.954
Chemical energy rate of combustion $\dot{Q}_{cc}$	Aspen Hysys	kW	307.42	336.23
	Aspen Plus			
	Ebsilon t_2 = var		307.45	336.1
	Ebsilon t_2 = const			
Net efficiency (η_{net})	Aspen Hysys	%	44.00	43.32
	Aspen Plus		43.88	43.05
	Ebsilon t_2 = var		43.07	42.8
	Ebsilon t_2 = const		44.16	43.12
Gross efficiency (η_g)	Aspen Hysys	%	50.21	48.01
	Aspen Plus		50.16	47.81
	Ebsilon t_2 = var		49.23	47.55
	Ebsilon t_2 = const		50.32	47.86

3.3. N_2, NO, N_2O and NO_2 Formation and Influence on Temperature

This subsection is intended to indicate the effect of the ammonia combustion reaction on the temperature in the combustion chamber. Due to the fact that Ebsilon is mainly adapted to flow analyses with less flexibility in setting combustion data, this subsection is mainly based on results from Aspen Plus and Aspen Hysys. General chemical reactions in ammonia combustion are as follows:

$$4NH_3 + 3O_2 \rightarrow 2N_2 + 6H_2O \quad (11)$$

$$4NH_3 + 5O_2 \rightarrow 4NO + 6H_2O \quad (12)$$

$$4NH_3 + 7O_2 \rightarrow 4NO_2 + 6H_2O \quad (13)$$

$$2NH_3 + 2O_2 \rightarrow N_2O + 3H_2O \quad (14)$$

In Ebsilon, the basic reaction is the conversion of ammonia to nitrogen according to reaction (11). Aspen Plus, on the other hand, assigns the basic reaction to the conversion of ammonia to nitric oxide according to stoichiometric Equation (12), by default. However, due to the fact that different results are obtained in Tables 7 and 9, it was worthwhile to trace the other possibilities for the conversion of ammonia in the presence of oxygen and hence a set of (14) equations.

HYSYS calculates and displays the heat of reactions in the reaction heat cell. Table 10 depicts the reaction heat of different mentioned reactions. In this case, all of the reaction heat cells are negative, indicating that the reaction produces heat (exothermic). In thermodynamics, the term exothermic process describes a process or reaction that releases energy from the system to its surroundings, usually in the form of heat, but also in a form of light (e.g., a spark, flame, or flash), electricity (e.g., a battery), or sound (e.g., explosion heard

when burning hydrogen). So, reactions 11 to 14 release 3.2 × 10^5 (kJ/kgmol), 2.3 × 10^5 (kJ/kgmol), 2.8 × 10^5 (kJ/kgmol), and 2.8 × 10^5 (kJ/kgmol), respectively. It can be understood that if all of these reactions could occur, reaction 11 releases the highest value of energy. This would take precedence in comparison to other reactions. Meanwhile, it is assumed that, in combined reaction, including reactions of N_2, N_2O, NO, and NO_2, each reaction is with ammonia conversion factor of 0.25.

Table 10. reaction heat for different reactions obtained by Hysys.

Reactions	Heat of Reaction *, kJ/kgmol
$4NH_3 + 3O_2 \rightarrow 2N_2 + 6H_2O$	-3.2×10^5
$4NH_3 + 5O_2 \rightarrow 4NO + 6H_2O$	-2.3×10^5
$4NH_3 + 7O_2 \rightarrow 4NO_2 + 6H_2O$	-2.8×10^5
$2NH_3 + 2O_2 \rightarrow N_2O + 3H_2O$	-2.8×10^5

* at 25 °C.

The effect of an ammonia combustion reaction on the temperature is shown in Table 11. It shows the results obtained with Aspen Plus and Aspen Hysys. On the basis of the given chemical reactions and the obtained results of temperature and elemental compositions downstream of the combustion chamber, it should be concluded that the highest energy effect accompanies the formation of NO_2, followed by the formation of N_2 and N_2O, successively, and the lowest temperature is downstream of the combustion chamber after the formation of NO.

Table 11. 18 g/s mixture 1 (syngas) with NH_3 combustion to NO, NO_2, N_2, N_2O under stoichiometric conditions (100 g/s exhaust).

Parameter	Symbol	Unit	Combined *	N_2	N_2O	NO	NO_2
Temperature at the WCC outlet t_2 = var	Aspen Hysys	°C	1107	1106	1104	1100	1116
	Aspen Plus		1106	1105	1103	1100	1115
	Ebsilon		n.a.	1100	n.a.	n.a.	n.a.
Fuel mass flow ($\dot{m}_{1-fuel}$)	Aspen Hysys Aspen Plus Ebsilon	g/s	18.00				
Oxygen mass flow ($\dot{m}_{1-O2}$)	Aspen Hysys	g/s	23.13	22.72	22.96	23.19	23.66
	Aspen Plus		23.13	22.72	22.96	23.19	23.66
	Ebsilon		n.a.	22.4	n.a.	n.a.	n.a.
Water mass flow ($\dot{m}_{1-H2O}$)	Aspen Hysys	g/s	58.86	59.28	59.04	58.80	58.33
	Aspen Plus		58.86	59.28	59.04	58.80	58.33
	Ebsilon		n.a.	59.6	n.a.	n.a.	n.a.
Exhaust temperature after HE (t_5)	Aspen Hysys	°C	187.9	186.1	186.3	183.60	195.00
	Aspen Plus		187.33	185.57	185.81	183.55	194.44
	Ebsilon		n.a.	147.3	n.a.	n.a.	n.a.
Turbine power GT (N_{GT})	Aspen Hysys	kW	89.40	89.61	89.26	89.05	89.66
	Aspen Plus		89.58	89.79	89.44	89.25	89.85
	Ebsilon		n.a.	89.53	n.a.	n.a.	n.a.
Turbine power GT^{bap} (N_{GT-bap})	Aspen Hysys	kW	65.46	65.58	65.37	65.14	65.75
	Aspen Plus		65.23	65.35	65.13	64.92	65.53
	Ebsilon		n.a.	65.2	n.a.	n.a.	n.a.
Combined turbines gross power (N_t)	Aspen Hysys	kW	154.9	155.2	154.6	154.2	155.4
	Aspen Plus		154.8	155.1	154.6	154.2	155.4
	Ebsilon		n.a.	154.72	n.a.	n.a.	n.a.
Power for own needs	Aspen Hysys	kW	19.03	18.94	18.99	19.05	19.15

(N_{cp})	Aspen Plus		19.28	19.19	19.25	19.30	19.40
	Ebsilon		n.a.	18.94	n.a.	n.a.	n.a.
Chemical energy rate of combustion ($\dot{Q}_{CC}$)	Aspen Hysys	kW			307.49		
	Aspen Plus						
	Ebsilon				307.45		
Net efficiency (η_{net})	Aspen Hysys	%	44.18	44.32	44.12	43.96	44.32
	Aspen Plus		44.08	44.21	44.01	43.86	44.22
	Ebsilon		n.a.	44.16	n.a.	n.a.	n.a.
Gross efficiency (η_g)	Aspen Hysys	%	50.37	50.48	50.30	50.16	50.55
	Aspen Plus		50.35	50.45	50.27	50.14	50.53
	Ebsilon		n.a.	50.32	n.a.	n.a.	n.a.
N_2 mass flow	Aspen Hysys	g/s	0.10	0.41			
	Aspen Plus		0.10	0.41	-	-	-
	Ebsilon		n.a.	0.31			
N_2O mass flow	Aspen Hysys	g/s	0.16		0.65		
	Aspen Plus		0.16	-	0.65	-	-
	Ebsilon		n.a.		n.a.		
NO mass flow	Aspen Hysys	g/s	0.22			0.89	
	Aspen Plus		0.22	-	-	0.89	-
	Ebsilon		n.a.			n.a.	
NO_2 mass flow	Aspen Hysys	g/s	0.34				1.36
	Aspen Plus		0.34	-	-		1.36
	Ebsilon		n.a.				n.a.

* Combined—each reaction with ammonia conversion factor of 0.25 (0.25·4 = 1).

4. PFD with Spray Ejector Condenser

In Figure 6, the extended version of the "PFD0" cycle is presented, shown in the previous chapter. The developed cycle "PFD1" includes additionally fuel preparation and carbon capture storage (CCS) units. Fuel comes out from the gasifier (R) as a product of a thermochemical process transformation of supplied dry sewage sludge in the presence of a gasifying agent. The gasifying agent is released after GT with optional release from a carbon capture unit (CCU) at an ambient pressure, consisting of a mixture of steam and CO_2. The gasifying agent properties, such as content of CO_2, steam, and its temperature or pressure, can be controlled as required. An oxygen compressor (CO_2) is supplied from an air separation unit (ASU). A spray ejector condenser (SEC) sucks the exhaust from the heat exchanger 1 (HE1), while the motive fluid is supplied to SEC through the dedicated pump (PSEC).

The outlet mixture of condensed steam and moist CO_2 vapor from SEC is directed to the separator with heat exchanger 2 (S + HE2), where low temperature source (LTS) is supplied and separation of CO_2 takes place. Water from HE2 is directed to PH2O and PSEC, while excess water is discharged out of the plant. Humid CO_2 vapor from the separator is directed to the CCU whereby, after each CO_2 compressor 1 and 2 (CCO2-1 and CCO2-2), there are intercoolers heat exchangers 3 and 4 (HE3 and HE4) with decantation which are supplied with water supplied from PH2O. Water after heating in CCU is directed to WCC where it reaches supercritical conditions. A partial release of CO_2 vapor can be used as a gasifying agent to the gasifier (R) or to WCC to manipulate and obtain the desired chemical reactions pathway. CO_2 vapor is directed to CO_2 storage tank ($STCO_2$) or can be used for other processes, such as methanol production.

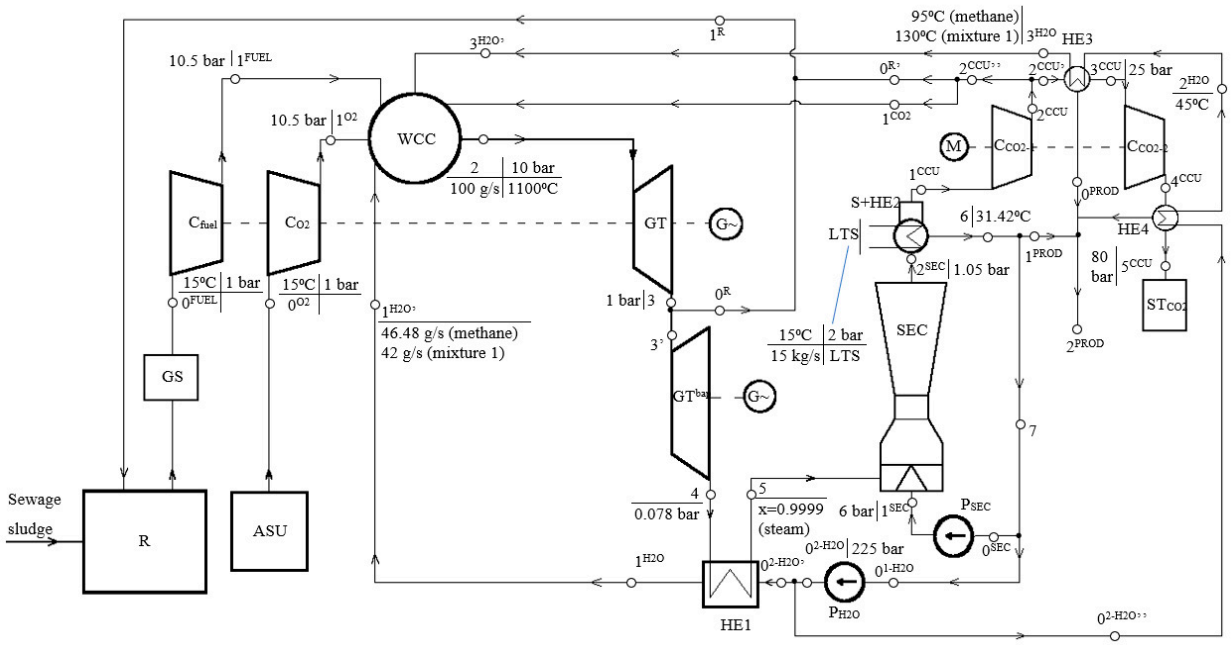

Figure 6. Process flow diagram of a gas mixture cycle—a steam-gas turbine system, where: WCC—wet combustion chamber; SEC—spray ejector condenser; R—gasifier (Reactor); GT—gas–steam turbine; GT^{bap}—gas–steam turbine—below ambient pressure; C_{fuel}—fuel compressor; C_{O2}—oxygen compressor; $C_{CO2-1,2}$—CO_2 capture unit compressors 1 and 2; P_{H2O}—water pump supplying supercritical water; P_{SEC}—water pump supplying SEC, S + HE2—separator with heat exchanger 2; HE 1, 3, and 4—heat exchanger 1, 3, and 4; ASU—air separation unit; GS—gas scrubber; G~—power generators; M—motor; LTS—low-temperature source, ST_{CO2}—CO_2 storage tank. Nodal points—general thermodynamic cycle: 0^{FUEL}, 0^{O2}, 1^{FUEL}, 1^{O2}, 2, 3, 3 ', 4, 5, 6, 7; optional: 2 '; CO_2 capture unit: 1^{CCU}, 2^{CCU}, 3^{CCU}, 4^{CCU}, 5^{CCU}; optional: $2^{CCU'}$, $2^{CCU''}$; SEC: 0^{SEC}, 1^{SEC}, 2^{SEC}; gasifying agent supply: 0^{R}; optional: $0^{R'}$,1^{R}; water production: 0^{PROD}, $1^{PROD'}$, 2^{PROD}; optional CO_2 injection to WCC: 1^{CO2}; water supply: $0^{1\text{-}H2O}$, $0^{2\text{-}H2O}$, $0^{2\text{-}H2O'}$, $0^{2\text{-}H2O''}$,1^{H2O}, 2^{H2O}, 3^{H2O}; optional: $1^{H2O'}$, $1^{H2O''}$, $3^{H2O'}$, $3^{H2O''}$.

The simulation models of "PFD1" developed in different computing codes are presented in Figures 7–9 (Aspen Hysys—Figure 7, Aspen Plus—Figure 8, Ebsilon—Figure 9), with most significant assumptions and calculated values in nodal points. Models do not contain the part connected with fuel preparation (gasifier and air separation unit). The main difference between models was approach to CCS part, especially with SEC modeling. The Ebsilon model (Figure 9) uses a spray ejector component, whereas other cycles define SEC operation through indirect models (direct-contact heat exchanger model, as shown in Figures 7 and 8). Moreover, cycles have a different arrangement of circulating water, which is extracted from exhaust gases. Next, through various configuration systems of heat exchanger, pumps are directed to WWC or SEC. One of the differences of simulation between Aspen Hysys and Plus is to consider decantation of heat exchangers. More accurately, separators are assumed in Aspen Hysys for decantation of heat exchangers, named decantation 1 and decantation 2, as seen in Figure 7.

In addition, although five reactions are available for mixture 1 fuel as a default in Aspen Plus, there is a need to define these five reactions in Aspen Hysys.

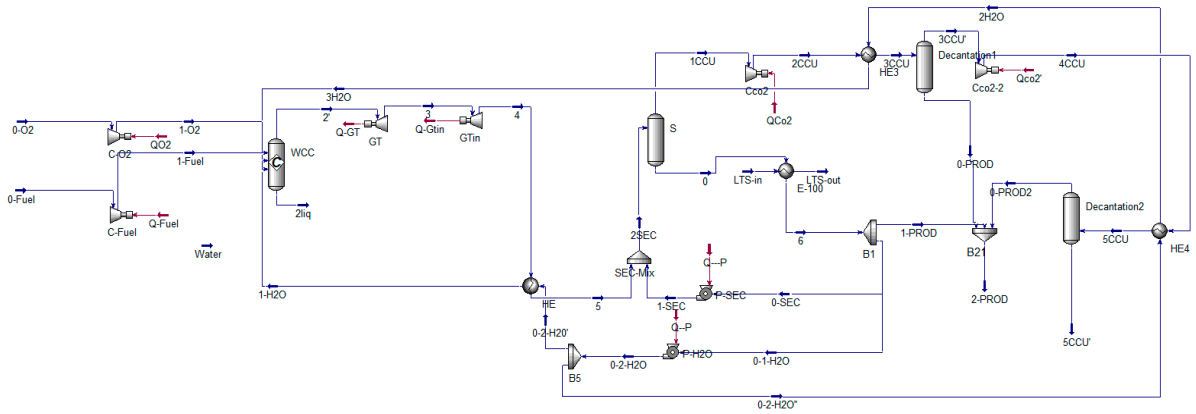

Figure 7. Simulation of PFD1 by Aspen HYSYS.

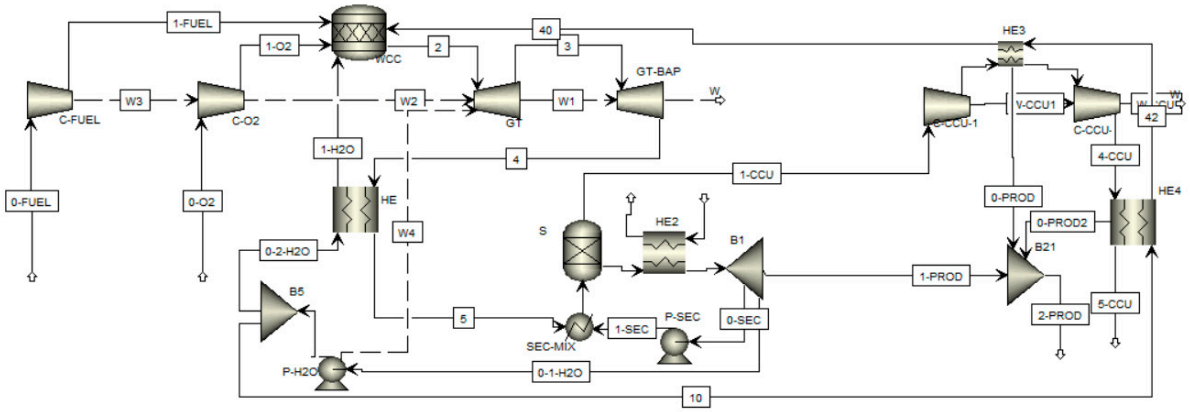

Figure 8. Simulation of PFD1 by Aspen Plus.

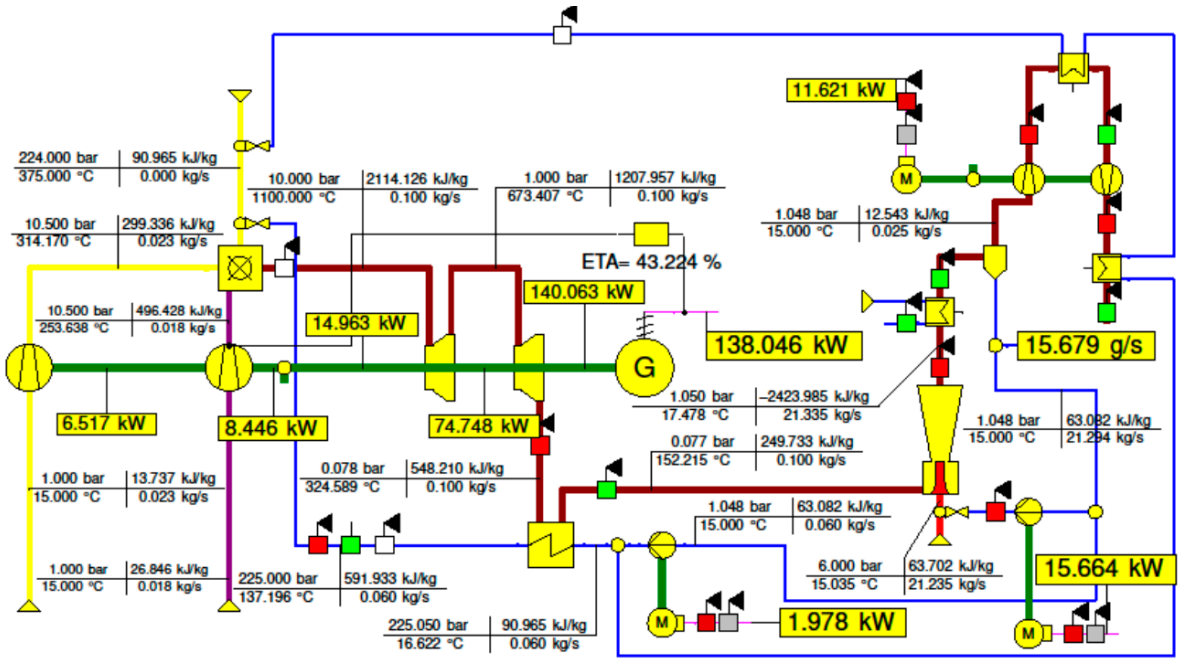

Figure 9. Simulation of PFD1 by by Ebsilon.

Subsection

A power plant design based on "PFD1" presented in this paper supplied with mixture 1 syngas fuel is assumed to be the target operation configuration. Table 12 shows the results in the case of Aspen Plus and Aspen Hysys for 10 bar and 1100 °C in WCC, and a comparison with methane. However, for Ebsilon, it is presented with a temperature lower than 1100 °C due to the fact that a higher level of similarities in efficiency was obtained.

Table 12. Results for mixture 1 and methane—"PFD1"—summary table.

Parameter	Symbol	Unit	Value Aspen Plus		Value Aspen HYSYS		Value Ebsilon	
Fuel type	—	-	Mixture 1	Methane	Mixture 1	Methane	Mixture 1	Methane
Fuel mass flow	$\dot{m}_{1-fuel}$	g/s	16.68	6.23	16.68	6.23	16.68	6.23
Oxygen mass flow	$\dot{m}_{1-O_2}$	g/s	21.21	24.86	21.21	24.86	20.76	24.85
Water mass flow	$\dot{m}_{1-H_2O}$	g/s	62.11	68.91	62.11	68.91	62.56	68.92
CO_2 mass flow in exhaust	$\dot{m}_{2-CO_2}$	g/s	22.68	17.10	22.68	17.10	22.68	17.09
NO mass flow in exhaust	$\dot{m}_{2-NO}$	g/s	0.82	-	0.82	-	-	-
Water mass flow in exhaust	$\dot{m}_{2-H_2O}$	g/s	76.50	82.90	76.50	82.90	76.93	82.91
Water production	$\dot{m}_{p-H_2O}$	g/s	14.38	14.00	14.38	14.00	14.226	13.876
Exhaust temperature (before regenerative HE1, after GT^{bap})	t_4	°C	322.11	317.95	321.4	317.1	288.0	283.04
Exhaust temperature (after regenerative HE1, x = 0.9999)	t_5	°C	41.83	41.83	38.95	39.73	38.95	39.73
Turbine power GT	N_{GT}	kW	90.3	94.0	91.05	95.38	86.00	89.168
Turbine power GT^{bap}	N_{GT-bap}	kW	65.6	68.0	66.14	69.04	62.16	64.19
Combined turbines gross power	N_t	kW	155.9	162.0	157.19	164.42	148.16	153.358
Optimistic SEC Pump power consumption (x = 0 in mixing part of SEC)	$N_{P-SEC,o}$	kW	17.79	12.94	17.79	12.89		
Not optimistic SEC Pump power consumption (x = 0.25 in mixing part of SEC)	$N_{P-SEC,n}$	kW	54.93	53.19	54.93	53.18	14.57	14.84
Power for own needs with optimistic SEC	$N_{cp,o}$	kW	43.61	32.49	43.59	32.62	41.22	35.612
Power for own needs with optimistic SEC	$N_{cp,no}$	kW	80.75	72.74	80.63	72.91		
Chemical energy rate of combustion	$\dot{Q}_{CC}$	kW	284.86	311.82	284.88	311.72	284.97	311.59
Net efficiency with optimistic SEC	$\eta_{net,o}$	%	39.43	41.54	39.91	41.58	37.53	37.8
Net efficiency with not optimistic SEC	$\eta_{net,no}$	%	26.40	28.63	26.87	28.66		
Gross efficiency	η_g	%	54.74	51.96	55.18	52.10	52.00	49.22

Figures 10 and 11 show the graphs plotted for combined turbines power, chemical rate of combustion, CO_2 fraction, exhaust water fraction, water production, and gross efficiency for mixture 1 and methane obtained from various computing codes, such as Aspen Plus, Aspen Hysys, and Ebsilon. The maximum combined power generated by turbines is 164.42 kW from methane at the mass flow of water 14.0 g/s obtained from Aspen Hysys. The minimum combined power generated by turbines is 148.16 kW from mixture 1 at the mass flow of water 14.226 g/s produced due to combustion. This result was obtained from Ebsilon. In Figure 11, the maximum combined power generated by turbines is 164.42 kW from methane at CO_2 in the exhaust of 17.1% mass obtained from Aspen Hysys. The minimum combined power generated by turbines is 148.16 kW from mixture 1 at CO_2 in the exhaust of 22.68% mass obtained from calculation in Ebsilon. Combined turbine power output was much higher in case of methane combustion in all computing codes. However, the power output obtained by thermodynamic analyses in Ebsilon was obtained at a lower level because the temperature of the beginning of the expansion started from a lower level. The CO_2 and H_2O content change depends on fuel composition in different ways. Thus, the relationship between the power output obtained and the composition of the flue gases composition that flow through its successive stages becomes apparent.

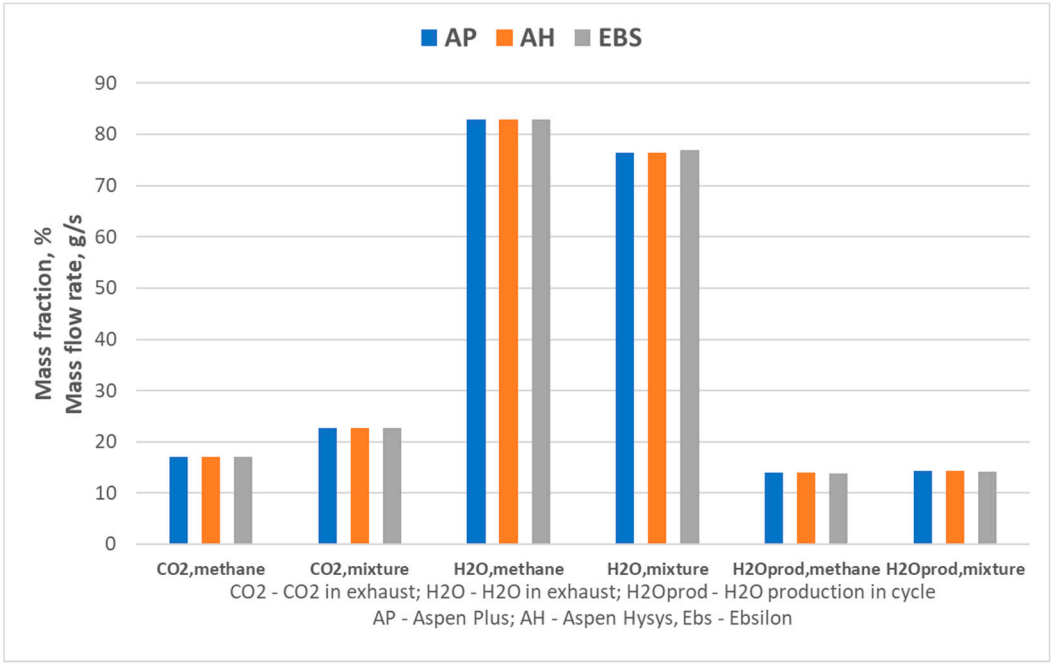

Figure 10. Exhaust CO_2, H_2O fraction and mass flow of water production in the cycle for various computing codes (AP—Aspen Plus, AH—Aspen Hysys, Ebs—Ebsilon).

The graphs in Figure 11 are plotted for chemical rate of combustion, combined power, and gross efficiency for mixture 1 and methane from Aspen Plus, Aspen Hysys, and Ebsilon, respectively. It should be noted that the results obtained from Aspen Plus and Aspen Hysys indicate the same values. The chemical energy rate of combustion was similar in the case of Ebsilon software.

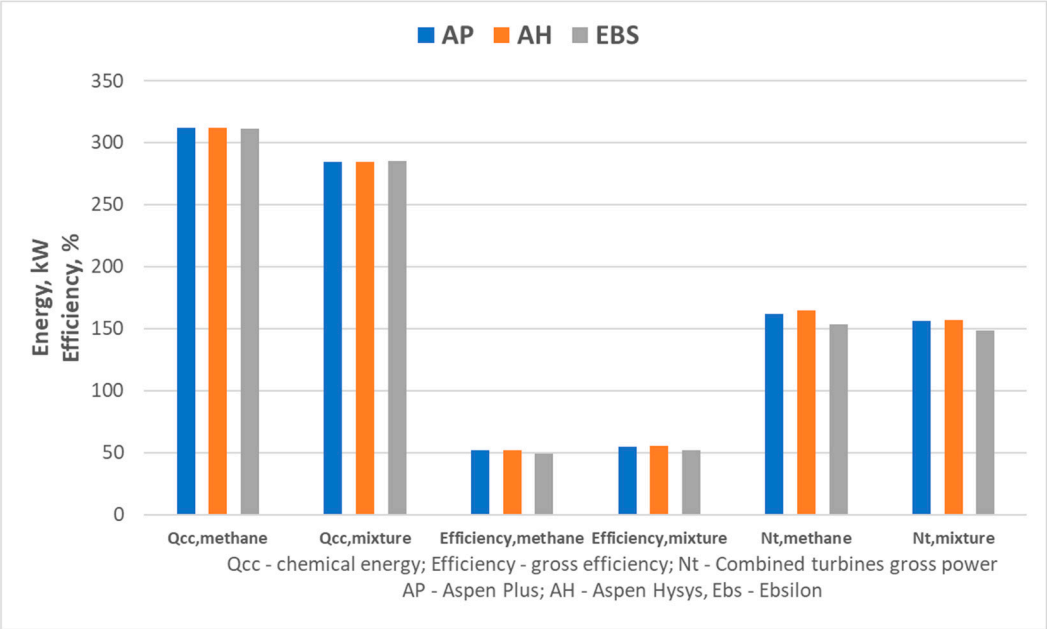

Figure 11. Combined turbine power, chemical energy of mixture 1 and methane combustion, and gross efficiency for various computing codes (AP—Aspen Plus, AH—Aspen Hysys, Ebs—Ebsilon).

The highest efficiency was calculated for mixture 1 in Apen Plus and Aspen Hysys (similar values, respectively: 54.74% and 55.18%). Lower efficiencies were achieved in the case of the Ebsilon computing code (52.00% for mixture 1 and 49.22% for methane).

For gross efficiency, there is a similar relationship for turbine power output, but additionally the chemical energy rate of the fuel is taken into account, which ultimately results in higher efficiencies for flue gases with increased steam production. A similar trend is observed for increased CO_2 in the flue gas. Thus, in order to clearly determine the effect of the fuel mixture on the performance of turbine and the entire nCO2PP cycle, a wider range of fuels would have to be studied—but this was not the purpose of the paper. First of all, it should be stated that there is a slight influence of the software used on the results obtained, but the basic tendencies are the same, which makes it possible to analyze various types of thermodynamic cycles.

The values of fuel mass flow, oxygen mass flow, and water mass flow of mixture 1 (syngas) and methane used in Aspen Plus and Aspen HYSYS are the same, but are a not so different from the values used in Ebsilon. So, this impacts the simulation of process flow diagram 1 ("PFD1") and the values obtained in Ebsilon is comparatively different from the values obtained from Aspen Plus and Aspen HYSYS. There are several reasons why the results may not be exactly the same. Firstly, there are some differences regarding simulation models, and procedures adopted inside the model preparation.

In calculations using the model developed thanks to the Ebsilon software (Figure 9), the first assumption is the mass flow rate of fuel together with an assumption of stoichiometric combustion inside WCC. Next, the amount of oxygen is calculated. The mass flow rate exhaust gases depends on the amount of cooling water to combustion chamber which is equal to 100 g/s. Based on this procedure and assumptions, nodal values in the thermal cycle can be computed.

Another difference in simulation between Ebsilon, Aspen Hysys, and Plus is SEC. An operating principle of the spray ejector condenser (SEC) shown in Figure 12 is described as follows.

Motive fluid in subsonic flow enters the nozzle (1^{SEC}) in Figure 12, which has a decreasing cross section area in which motive fluid is accelerated, while pressure energy is converted to velocity energy. Sonic flow velocity is reached at the same time when a min-

imum area of the nozzle (1^{SEC}) is reached. In supersonic flow, the nozzle (1^{SEC}) is an increasing area device. Entrained fluid (5) enters the suction chamber (b) and increases its velocity. The motive fluid and entrained fluid (5-MC) mix together in a mixing chamber (a-c). The mixture is directed to diffuser—throat (c) in supersonic flow in a decreasing area. The diffuser (c-2^{SEC}) in subsonic flow has an increasing area and converts velocity energy to pressure energy. The proper design of SEC is important for the feasibility in operation for a particular case of required conditions. Basically, ejectors are designed using a lot of empirical correlations and any information related to their design is not available in the public domain. It would be recommended to rely on the design characteristics.

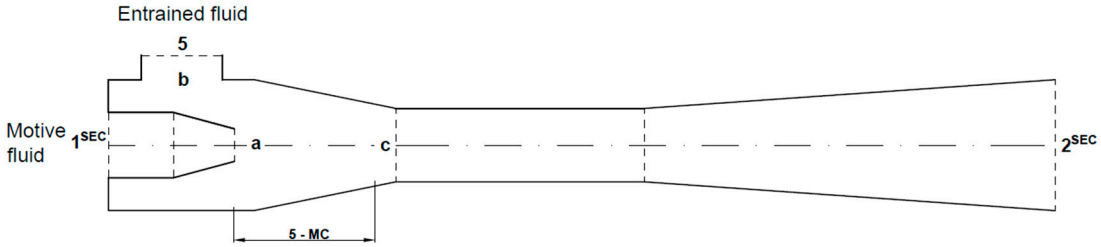

Figure 12. Spray ejector condenser 1^{SEC}: Nozzle inlet, a: Nozzle outlet, a–c: Mixing chamber, b: Suction chamber, c: Throat (part of Diffuser), c-2^{SEC}: Diffuser, 5 Inlet of entrained fluid, 5-MC: Entrained fluid in mixing chamber.

In order to improve the design, efficiency, and feasibility of SEC, similar characteristics could be obtained using CFD calculations and data from laboratory experiments for the purposes of the paper. Elongation of the nozzle part can possibly contribute to an increase in efficiency. Because of high compression ratio, further research has to be conducted to decide whether a single configuration or several ejectors in multiple stages, and vertical or horizontal alignment of an ejector, would be preferred.

In this study, the motive fluid has to be H_2O (1^{SEC}) while the entrained fluid (5) is the mixture of CO_2 and H_2O. Both $CO_2$and H_2O occupy a large volume, causing a decrease in efficiency. For the optimum case with novel approach steam, H_2O would immediately be condensed (5-MC) in mixing chamber of SEC, contributing to an increase in efficiency at the same time, but in the less favorable case steam would be partially condensed in SEC, resulting in a decrease in efficiency due to the increase in a required motive fluid mass flow.

Although the ejector was available in Ebsilon for a simulation of SEC, the mixer was used in Aspen Hysys and Plus due to lack of ejector in mentioned software. So, the desired results of water when used in mixer are obtained according to Equation (15).

$$\chi = \frac{\dot{V}_{5-MC}}{\dot{V}_{1^{SEC}}}, - \quad (15)$$

where χ is volumetric entrainment ratio considered. $V_{5\text{-}MC}$ demonstrates suction gas–fluid volume flow to the mixing chamber of SEC (m^3/s) and $V_{1^{SEC}}$ is the motive fluid volume flow (m^3/s).

Moreover, the assumptions concerning fuels were a little different (low heating value, fuel inlet composition). This was because computing codes used various physical tables regarding fuel properties. The iterative method of calculating the problem also seems to be a crucial factor.

5. Negative Emission Power Plant Effect

Currently, sewage sludge is considered as a biomass, according to the new Polish Act on Renewable Energy Sources of 20 February 2015 and its novel version of 19 July 2019. The possibility to utilize sewage sludge in gasification process is an additional advantage of the proposed solution. A comparison of the emissivity of the systems for the different

options presented in this report is summarized in Table 13. Of the parameters listed in the table, two which determine carbon dioxide emissions are especially noteworthy, namely:

$$eCO_2 = \frac{\dot{m}_{2-CO2}}{N_t - N_{cp}} 3600 \quad (16)$$

$$\eta_{net} \cdot eCO_2 = \frac{N_t - N_{cp}}{\dot{Q}_{CC}} \frac{\dot{m}_{2-CO2}}{N_t - N_{cp}} 3600 = \frac{\dot{m}_{2-CO2}}{\dot{Q}_{CC}} 3600 \quad (17)$$

Negative emissions of CO_2 were counted based on two parameters defined in Equations (15) and (16). Firstly, in (15), the specific CO_2 emission is given, which is the quotient of the CO_2 capture mass flow rate with respect to the net power. The net power was classically defined as the difference in the turbine-generated power N_t and the demand power N_{cp}. This definition is also found in the works of authors, such as [57] or [58], in relation to cycles with CO_2 capture. Secondly, Equation (16) defines the product of the efficiency of the whole cycle and the specific CO_2 emitted. Additionally, after simplification, this parameter directly expresses the relative emissivity related to the chemical energy rate. In a traditional view, both parameters (Equations (15) and (16)) show the emissions of the unit, but in the case of nCO2PP they are an indicator of the negative emissions related to the electrical energy obtained from the cycle or to the chemical energy supplied to the cycle, respectively. The results in Table 13 were selected for Aspen Plus and Hysys as the least optimistic of the previous results in Section 4.

Table 13. Negative emission power plant effect—results for Aspen Plus.

Parameter	Software	Symbol	Unit	Methane PP -Conventional	Methane PFD with SEC Zero-Emission	Mixture PFD with SEC nCO₂PP
Net efficiency with optimistic SEC	Aspen Plus	η_{net}	%	47.1	41.5	39.4
	Aspen Hysys			47.1	41.5	39.9
CO_2 mass flow in exhaust	Aspen Plus	$\dot{m}_{2-CO2}$	g/s	17.1	17.1	22.7
	Aspen Hysys			17.1	17.1	22.7
Power for own needs with optimistic SEC	Aspen Plus	N_{cp}	kW	15.0	32.5	43.6
	Aspen Hysys			15.0	32.6	43.6
Turbine power output	Aspen Plus	N_t	kW	162.0	162.0	155.9
	Aspen Hysys			162.0	164	157.1
Chemical energy rate of combustion	Aspen Plus	$\dot{Q}_{CC}$	kW	311.8	311.8	284.9
	Aspen Hysys			311.8	311.8	284.9
Emission of carbon dioxide	Aspen Plus	eCO_2	kg/MWh	418.78	0.0	−727.12
	Aspen Hysys			418.78	0.0	−720.0
Relative emissivity of carbon dioxide	Aspen Plus	$\eta_{net} \cdot eCO_2$	%kg/MWh	197.42	0.0	−286.70
	Aspen Hysys			197.42	0.0	−286.70
Avoided emission of carbon dioxide	Aspen Plus	Avoid eCO_2	kg/MWh	0.00	475.33	1454.23
	Aspen Hysys			0.00	476.22	1440

Avoided relative emissivity of carbon dioxide	Aspen Plus	Avoid $\eta_{net} \cdot eCO_2$	%kg/MWh	0.00	197.45	573.40
	Aspen Hysys			0.00	197.54	40.573
Specific Primary Energy Consumption for Carbone Avoided	Aspen Plus	*SPECCA*	MJ/kgCO_2	NA	0.999	0.822
	Aspen Hysys			NA	0.999	0.822

As shown in Table 13 in the conventional cycle where methane is burnt, the emissivity related to the electrical energy eCO_2 for both Aspen Plus and Hysys is 418.78 kg/MWh_{el} and, in case of emissivity related to the chemical energy, $\eta_{net} \cdot eCO_2$ is 197.42 kg/MW_{ch}. An additional set of equipment should be used to avoid carbon dioxide emissions. The emissions of CO_2, relative to the power output, for the combustion of methane in the novel power plant, outlined in this paper (Table 13), were slightly lower in comparison to the reference case used by Saari et al. [22] (482 kg/MWh_{el}). However, in terms of negative emissions achieved with producer gas from gasification of sewage sludge, the novel power plant concept significantly outperformed chemical looping with oxygen uncoupling (CLOU) plant, as proposed by Saari et al. [22] (13 kg/MWh_{el}). In the zero-carbon unit, on the other hand, we capture carbon dioxide and, thus, avoid emissivity related to the electrical energy at the level eCO_2 475.33 kg/MWh_{el} in Aspen Plus and 476.22 in Aspen Hysys and, in the case of emissivity related to the chemical energy, we avoid $\eta_{net} \cdot eCO_2$ 197.45 kg/MWch and 197.54 kg/MW in Aspen Plus and Hysys, respectively. In the case of nCO2PP, the indicated coefficients are much more favorable. Both parameters show that the avoided emissivity of the block after carbon dioxide capture is equal to twice the absolute value of the previously determined numbers. Consequently, the avoided emissivity value for nCO2PP is about three times higher than that for zero-emission units.

The specific power consumption associates to the modelled oxygen generating station (ASU) is β = 0.248 kWh/kgO_2 (for comparison, the value of the energy intensity in a study by Gou et al. [59] is β = 0.247 kWh/kgO_2, while, in a study by Liu et al. [60], it is β = 0.250kWh/kgO_2).

To compare plants which include different capture efficiencies, regeneration temperature, and electrical efficiencies penalties, the specific primary energy consumption for carbone avoided is introduced according to other works [57,58]. For research, MEA is classified at the level 4.16; however, Bonalumi et al. improved this parameter to value 2.86 and 2.58 for chilled (with salts) and cooled (without salts), respectively. In the presented case (Table 13), the SPECCA value reaches 0.999 and 0.822 for zero-emmision and negative emission power plant, respectively.

6. Effect of Specific Heat Capacity

The specific heat capacity (also simply specific heat) of a substance is the heat capacity per unit mass of that substance. Here, we shall discuss the specific heat capacity using SI units (kJ/kg·K). Heat capacity can be expressed at a constant volume (c_v) or constant pressure (c_p). Specific heat capacity of mixture 1 at a constant pressure and volume as a function of temperature from 1 °C to 1300 °C, calculated using Aspen Hysys, Aspen Plus, and Ebsilon, are presented in Figures 13 and 14, respectively.

It can be regarded that c_p and c_v are faced with a decreased trend from 1 °C to 200 °C, so that the minimum value of c_p and c_v is 1.78 kJ/kg·K and 1.32 kJ/kg·K at 200 °C, respectively. After that, they increase with rising the temperature. In addition, for T ≥ 200 °C, the specific heat capacity at constant volume (c_v) and constant pressure (c_p) remain approximately constant with increasing the pressure from 0.078 to 10 bar. Specific heat capacity (c_p) in nodal points for at 10 bar and 1100 °C for Aspen Hysys, Aspen Plus, and Ebsilon is represented. It may be viewed that the minimum value (0.92) of c_p belongs to oxygen, whilst the maximum one belongs to water (Figure 15). In addition, there is a direct relation

between increasing temperature and c_p. The specific heat capacity values extracted from the codes are close to each other, but when the processes in the individual devices are taken into account, they affect the efficiency values of the whole cycle, in both considered versions of the nCO2PP cycle.

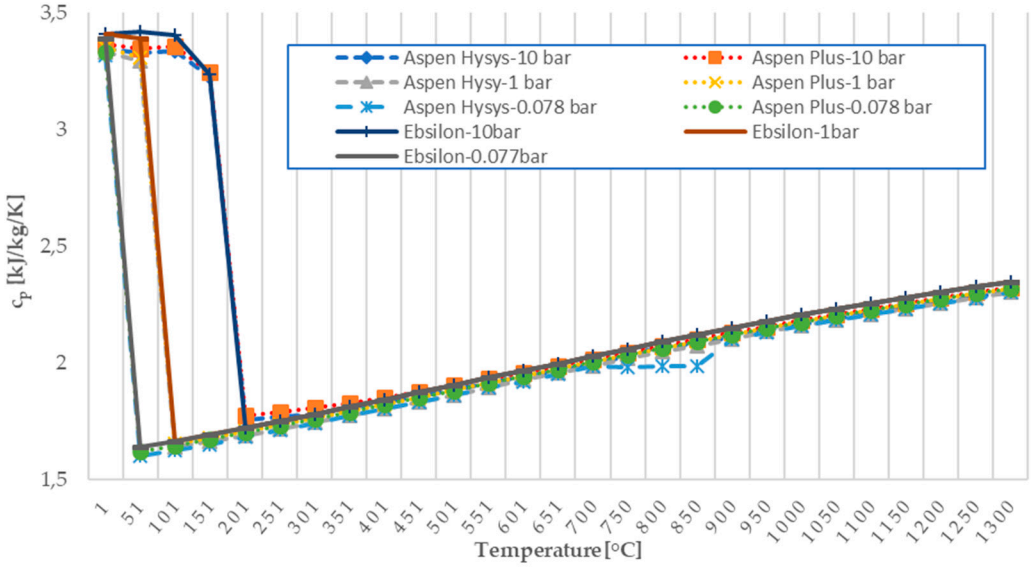

Figure 13. Distribution of heat capacity at constant pressure per temperature after WCC at different pressure in Aspen Hysys, Aspen Plus, and Ebsilon.

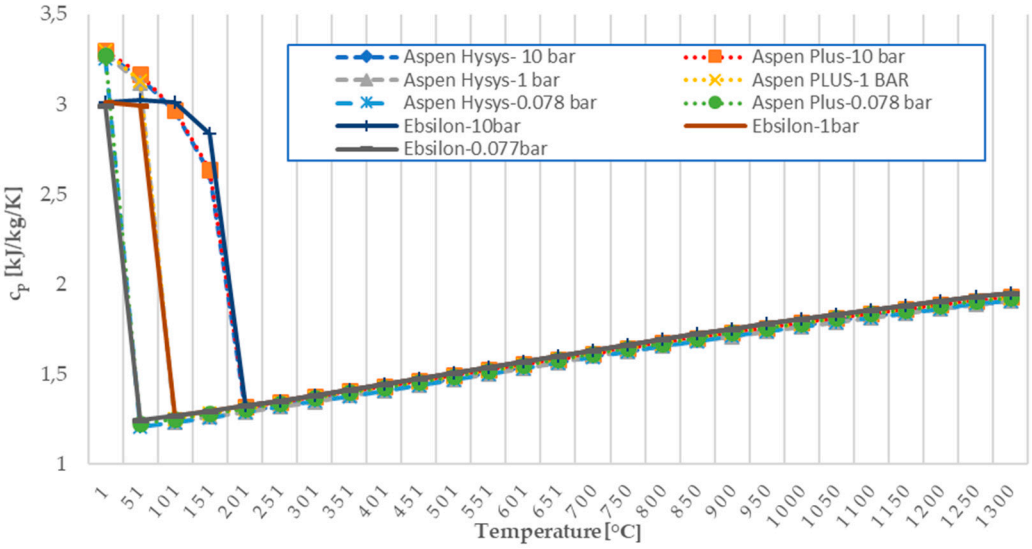

Figure 14. Distribution of heat capacity at constant volume per temperature after WCC at different pressure in Aspen Hysys, Aspen Plus and Ebsilon.

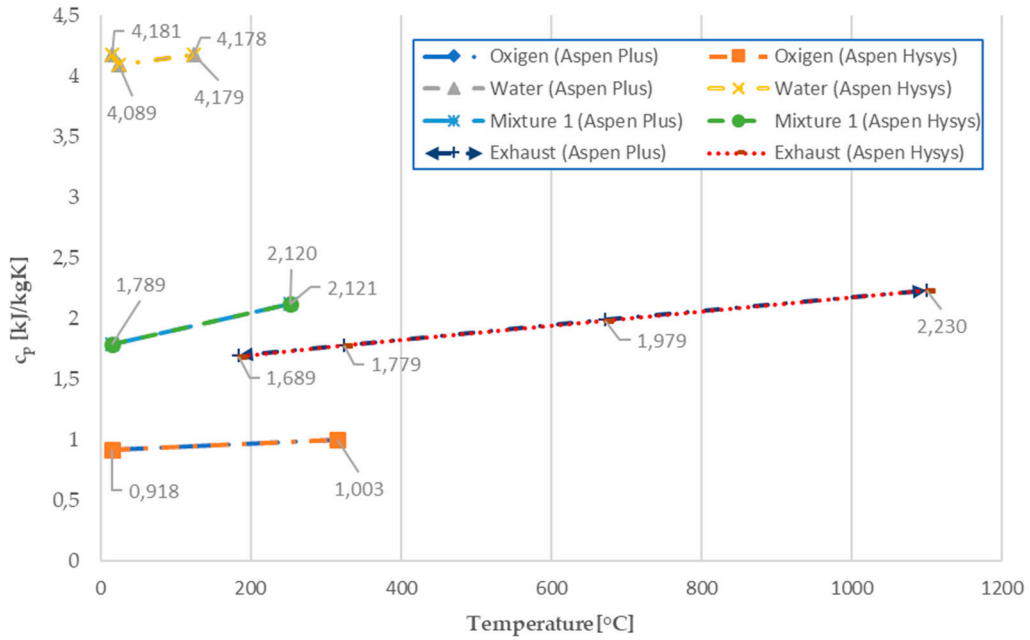

Figure 15. Specific heat capacity (c_p) in nodal points PFD0, mixture 1, WCC exhaust at 10 bar and 1100 °C for Aspen Hysys, Aspen Plus and Ebsilon.

7. Conclusions

The developed version of the cycle, called Process Flow Diagram 0 ("PFD0"), offered the possibility to perform a preliminary assessment of the main cycle parameters, generated power output, as well as temperature in the combustion chamber and at the turbine outlet. It could be concluded that the proposed design of the negative power plant could be considered feasible and competitive with other types BECCS plant, presented in the literature, especially when achievable negative emissions (−720 kg_{CO2}/MWh_{el}) are taken into the account.

On the basis of the obtained results, the following key conclusions can be presented:

(1) The presented cycle "PFD0" allows generating approx. 150 kW for mixture 1 and 160 kW for methane in three considered software (Table 9).

(2) When inflicting the same mass flow rates (oxygen, water, mixture 1, or methane) and temperatures as in Ebsilon at the inlet to the combustion chamber, we obtain a temperature higher by 27 or 9 degrees Celsius or more in Aspen Plus and Aspen Hysys, and therefore the temperature at the exit from the WCC is 1073 or 1091 °C.

(3) On the other hand, when given the same mass flow rates (oxygen, water, mixture 1 or methane) and different temperatures downstream of the heat exchanger in the Ebsilon, the temperature downstream of the combustion chamber can be constant, so the WCC plot is 1100 °C.

(4) The trend is similar for mixture 1 and methane, but the differences are greater as we do not have the same set of reactions concerning the combustion chamber. In this case, the conversion of the ammonia combustion reaction to NO and H_2O to combustion to N_2 and H_2O gives a gain of 6 degrees Celsius more (see Table 11). In mixture 1, we have significant ammonia content why explains the large difference with respect to combustion in traditional chambers, where this influence is negligible.

(5) An argument that a likely reason for the differences in the two codes are the different definitions, e.g., in one specific heat capacity of steam stabilized in Ebsilon and in Aspen specific heat capacity of steam following the P-R equation, is the fact that we obtain different temperatures after the pump and after the compressors with assumed isentropic efficiencies at the same level, at the same inlet temperatures, and at the same pressure rise (see Section 6).

Additionally, the proposed version of the cycle, called the process flow diagram 1 ("PFD1"), offered the possibility to perform a preliminary assessment of the main cycle parameters, consumed and generated powers, efficiencies, and temperatures in nodal points. The following conclusions can be drawn from Sections 4 and 5:

(1) SEC significantly affects the efficiency of the cycle but provides the opportunity for carbon dioxide separation in the nCO2PP system.
(2) Differences in the Aspen Plus, Aspen Hysys, and Ebsilon codes follow a similar trend.
(3) In subsequent calculations, the modeling of the injector should be approached more extensively. For example, there should be more reliance on measurement results obtained from one's own experiment.
(4) The possibility of a negative CO_2 emission power plant and the positive environmental impact of the proposed solution were demonstrated.

Author Contributions: Conceptualization, P.Z. and P.M.; methodology, P.Z. and P.M.; software, P.Z., P.M., M.A., K.S. and N.S.; validation, P.Z., P.M., H.P.-K., J.B. and D.M.; formal analysis, P.Z. and P.M.; investigation, P.Z., P.M., M.A., K.S. and N.S.; resources, P.Z. and P.M.; data curation, P.Z., P.M., M.A. and K.S.; writing—original draft preparation, P.Z., P.M., M.A., T.K., K.S. and N.S.; writing—review and editing, P.Z., P.M., H.P.-K., J.B., Ł.N. and D.M.; visualization, M.A., T.K., K.S.; supervision, H.P.-K., J.B., D.M.; project administration, D.M., P.Z., H.P-K. and P.M.; funding acquisition, D.M., P.Z. and P.M. All authors have read and agreed to the published version of the manuscript.

Funding: The research leading to these results has received funding from the Norway Grants 2014–2021 via the National Centre for Research and Development. Article has been prepared within the frame of the project: "Negative CO_2 emission gas power plant"—NOR/POLNORCCS/NEGATIVE-CO2-PP/0009/2019-00 which is co-financed by programme "Applied research" under the Norwegian Financial Mechanisms 2014–2021 POLNOR CCS 2019—Development of CO_2 capture solutions integrated in power and industry processes.

Conflicts of Interest: The authors declare no conflict of interest. The funders had no role in the design of the study; in the collection, analyses, or interpretation of data; in the writing of the manuscript, or in the decision to publish the results.

References

1. United Nations Framework Convention on Climate Change—Paris Agreement. Available online: https://unfccc.int/process-and-meetings/the-paris-agreement/the-paris-agreement (accessed on 1 July 2021).
2. Masson-Delmotte, V.; Zhai, P.; Pörtner, H.-O.; Roberts, D.; Skea, J.; Shukla, P.R.; Pirani, A.; Moufouma-Okia, W.; Péan, C.; Pidcock, R.; et al. *Global Warming of 1.5 °C*; IPCC—The Intergovernmental Panel on Climate Change: Geneva, Switzerland, 2019.
3. Friedlingstein, P.; Jones, M.W.; O'Sullivan, M.; Andrew, R.M.; Hauck, J.; Peters, G.P.; Peters, W.; Pongratz, J.; Sitch, S.; Le Quéré, C.; et al. Global Carbon Budget 2019. *Earth Syst. Sci. Data* **2019**, *11*, 1783–1838, https://doi.org/10.5194/essd-11-1783-2019.
4. Romanak, K.; Fridahl, M.; Dixon, T. Attitudes on Carbon Capture and Storage (CCS) as a Mitigation Technology within the UNFCCC. *Energies* **2021**, *14*, 629, https://doi.org/10.3390/en14030629.
5. Hiremath, M.; Viebahn, P.; Samadi, S. An Integrated Comparative Assessment of Coal-Based Carbon Capture and Storage (CCS) Vis-à-Vis Renewable Energies in India's Low Carbon Electricity Transition Scenarios. *Energies* **2021**, *14*, 262, https://doi.org/10.3390/en14020262.
6. Sifat, N.S.; Haseli, Y. A Critical Review of CO2 Capture Technologies and Prospects for Clean Power Generation. *Energies* **2019**, *12*, 4143, https://doi.org/10.3390/en12214143.
7. Qvist, S.; Gładysz, P.; Bartela, L.; Sowiżdżał, A. Retrofit Decarbonization of Coal Power Plants—A Case Study for Poland. *Energies* **2020**, *14*, 1, https://doi.org/10.3390/en14010120.
8. Gładysz, P.; Sowiżdżał, A.; Miecznik, M.; Hacaga, M.; Pająk, L. Techno-Economic Assessment of a Combined Heat and Power Plant Integrated with Carbon Dioxide Removal Technology: A Case Study for Central Poland. *Energies* **2020**, *13*, 2841, https://doi.org/10.3390/en13112841.
9. Gładysz, P.; Stanek, W.; Czarnowska, L.; Węcel, G.; Langørgen, Ø. Thermodynamic assessment of an integrated MILD oxyfuel combustion power plant. *Energy* **2017**, *137*, 761–774, https://doi.org/10.1016/j.energy.2017.05.117.
10. Gładysz, P.; Stanek, W.; Czarnowska, L.; Sładek, S.; Szlęk, A. Thermo-ecological evaluation of an integrated MILD oxy-fuel combustion power plant with CO2 capture, utilisation, and storage—A case study in Poland. *Energy* **2018**, *144*, 379–392, https://doi.org/10.1016/j.energy.2017.11.133.

11. Míguez, J.L.; Porteiro, J.; Pérez-Orozco, R.; Gómez, M. Technology Evolution in Membrane-Based CCS. *Energies* **2018**, *11*, 3153, https://doi.org/10.3390/en11113153.
12. Sieradzka, M.; Gao, N.; Quan, C.; Mlonka-Mędrala, A.; Magdziarz, A. Biomass Thermochemical Conversion via Pyrolysis with Integrated CO2 Capture. *Energies* **2020**, *13*, 1050, https://doi.org/10.3390/en13051050.
13. Cannone, S.F.; Lanzini, A.; Santarelli, M. A Review on CO_2 Capture Technologies with Focus on CO_2-Enhanced Methane Recovery from Hydrates. *Energies* **2021**, *14*, 387, https://doi.org/10.3390/en14020387.
14. Arora, A.; Kumar, A.; Bhattacharjee, G.; Kumar, P.; Balomajumder, C. Effect of different fixed bed media on the performance of sodium dodecyl sulfate for hydrate based CO 2 capture. *Mater. Des.* **2016**, *90*, 1186–1191, https://doi.org/10.1016/j.matdes.2015.06.049.
15. Arora, A.; Kumar, A.; Bhattacharjee, G.; Balomajumder, C.; Kumar, P. Hydrate-Based Carbon Capture Process: Assessment of Various Packed Bed Systems for Boosted Kinetics of Hydrate Formation. *J. Energy Resour. Technol.* **2020**, *143*, 033005, https://doi.org/10.1115/1.4048304.
16. Detz, R.J.; van der Zwaan, B. Transitioning towards negative CO_2 emissions. *Energy Policy* **2019**, *133*, 110938, https://doi.org/10.1016/j.enpol.2019.110938.
17. Lisbona, P.; Pascual, S.; Pérez, V. Evaluation of Synergies of a Biomass Power Plant and a Biogas Station with a Carbon Capture System. *Energies* **2021**, *14*, 908, https://doi.org/10.3390/en14040908.
18. Mendiara, T.; García-Labiano, F.; Abad, A.; Gayán, P.; de Diego, L.F.; Izquierdo, M.; Adánez, J. Negative CO2 emissions through the use of biofuels in chemical looping technology: A review. *Appl. Energy* **2018**, *232*, 657–684, https://doi.org/10.1016/j.apenergy.2018.09.201.
19. Bhui, B.; Vairakannu, P. Prospects and issues of integration of co-combustion of solid fuels (coal and biomass) in chemical looping technology. *J. Environ. Manag.* **2018**, *231*, 1241–1256, https://doi.org/10.1016/j.jenvman.2018.10.092.
20. Lyngfelt, A.; Johansson, D.J.; Lindeberg, E. Negative CO2 emissions - An analysis of the retention times required with respect to possible carbon leakage. *Int. J. Greenh. Gas Control* **2019**, *87*, 27–33, https://doi.org/10.1016/j.ijggc.2019.04.022.
21. Niu, X.; Shen, L.; Jiang, S.; Gu, H.; Xiao, J. Combustion performance of sewage sludge in chemical looping combustion with bimetallic Cu–Fe oxygen carrier. *Chem. Eng. J.* **2016**, *294*, 185–192, https://doi.org/10.1016/j.cej.2016.02.115.
22. Saari, J.; Peltola, P.; Tynjälä, T.; Hyppänen, T.; Kaikko, J.; Vakkilainen, E. High-Efficiency Bioenergy Carbon Capture Integrating Chemical Looping Combustion with Oxygen Uncoupling and a Large Cogeneration Plant. *Energies* **2020**, *13*, 3075, https://doi.org/10.3390/en13123075.
23. Buscheck, T.A.; Upadhye, R.S. Hybrid-energy approach enabled by heat storage and oxy-combustion to generate electricity with near-zero or negative CO2 emissions. *Energy Convers. Manag.* **2021**, *244*, 114496, https://doi.org/10.1016/j.enconman.2021.114496.
24. Pawlak-Kruczek, H.; Niedzwiecki, L.; Ostrycharczyk, M.; Czerep, M.; Plutecki, Z. Potential and methods for increasing the flexibility and efficiency of the lignite fired power unit, using integrated lignite drying. *Energy* **2019**, *181*, 1142–1151, https://doi.org/10.1016/j.energy.2019.06.026.
25. Madejski, P.; Żymełka, P. Calculation methods of steam boiler operation factors under varying operating conditions with the use of computational thermodynamic modeling. *Energy* **2020**, *197*, 117221, https://doi.org/10.1016/j.energy.2020.117221.
26. Modliński, N.; Szczepanek, K.; Nabagło, D.; Madejski, P.; Modliński, Z. Mathematical procedure for predicting tube metal temperature in the second stage reheater of the operating flexibly steam boiler. *Appl. Therm. Eng.* **2019**, *146*, 854–865, https://doi.org/10.1016/j.applthermaleng.2018.10.063.
27. Mączka, T.; Pawlak-Kruczek, H.; Niedzwiecki, L.; Ziaja, E.; Chorążyczewski, A. Plasma Assisted Combustion as a Cost-Effective Way for Balancing of Intermittent Sources: Techno-Economic Assessment for 200 MW_{el} Power Unit. *Energies* **2020**, *13*, 5056, https://doi.org/10.3390/en13195056.
28. Benato, A.; Bracco, S.; Stoppato, A.; Mirandola, A. LTE: A procedure to predict power plants dynamic behaviour and components lifetime reduction during transient operation. *Appl. Energy* **2016**, *162*, 880–891, https://doi.org/10.1016/j.apenergy.2015.10.162.
29. Capron, M.; Stewart, J.; N'Yeurt, A.D.R.; Chambers, M.; Kim, J.; Yarish, C.; Jones, A.; Blaylock, R.; James, S.; Fuhrman, R.; et al. Restoring Pre-Industrial CO_2 Levels While Achieving Sustainable Development Goals. *Energies* **2020**, *13*, 4972, https://doi.org/10.3390/en13184972.
30. Cheng, F.; Small, A.A.; Colosi, L.M. The levelized cost of negative CO2 emissions from thermochemical conversion of biomass coupled with carbon capture and storage. *Energy Convers. Manag.* **2021**, *237*, 114115, https://doi.org/10.1016/j.enconman.2021.114115.
31. EU Carbon Price Hits Record 50 Euros per Tonne on Route to Climate Target | Reuters. Available online: https://www.reuters.com/business/energy/eu-carbon-price-tops-50-euros-first-time-2021-05-04/ (accessed on 7 August 2021).
32. Restrepo-Valencia, S.; Walter, A. Techno-Economic Assessment of Bio-Energy with Carbon Capture and Storage Systems in a Typical Sugarcane Mill in Brazil. *Energies* **2019**, *12*, 1129, https://doi.org/10.3390/en12061129.
33. Mikielewicz, D.; Wajs, J.; Ziółkowski, P.; Mikielewicz, J. Utilisation of waste heat from the power plant by use of the ORC aided with bleed steam and extra source of heat. *Energy* **2016**, *97*, 11–19, https://doi.org/10.1016/j.energy.2015.12.106.
34. Szablowski, L.; Krawczyk, P.; Badyda, K.; Karellas, S.; Kakaras, E.; Bujalski, W. Energy and exergy analysis of adiabatic compressed air energy storage system. *Energy* **2017**, *138*, 12–18, https://doi.org/10.1016/j.energy.2017.07.055.

35. Bartela, L.; Skorek-Osikowska, A.; Kotowicz, J. Economic analysis of a supercritical coal-fired CHP plant integrated with an absorption carbon capture installation. *Energy* **2014**, *64*, 513–523, https://doi.org/10.1016/j.energy.2013.11.048.
36. Zymelka, P.; Szega, M.; Madejski, P. Techno-Economic Optimization of Electricity and Heat Production in a Gas-Fired Combined Heat and Power Plant with a Heat Accumulator. *J. Energy Resour. Technol.* **2020**, *142*, 022101, https://doi.org/10.1115/1.4044886.
37. Kotowicz, J.; Job, M.; Brzęczek, M. The characteristics of ultramodern combined cycle power plants. *Energy* **2015**, *92*, 197–211, https://doi.org/10.1016/j.energy.2015.04.006.
38. Topolski, J.; Badur, J. Efficiency of HRSG within a Combined Cycle with gasification and sequential combustion at GT26 Turbine. In Proceedings of the Second International Scientific Symposium Compower, Gdańsk, Poland, 4–7 September 2000; pp. 291–298.
39. Ziółkowski, P.; Badur, J.; Ziółkowski, P. An energetic analysis of a gas turbine with regenerative heating using turbine extraction at intermediate pressure - Brayton cycle advanced according to Szewalski's idea. *Energy* **2019**, *185*, 763–786, https://doi.org/10.1016/j.energy.2019.06.160.
40. Głuch, J. Selected problems of determining an efficient operation standard in contemporary heat-and-flow diagnostics. *Pol. Marit. Res.* **2009**, *16*, 22–26, https://doi.org/10.2478/v10012-008-0040-6.
41. Ong'Iro, A.; Ugursal, V.; Al Taweel, A.; Lajeunesse, G. Thermodynamic simulation and evaluation of a steam CHP plant using ASPEN Plus. *Appl. Therm. Eng.* **1996**, *16*, 263–271, https://doi.org/10.1016/1359-4311(95)00071-2.
42. Liu, B.; Yang, X.-M.; Song, W.-L.; Lin, W.-G. Process simulation of formation and emission of NO and N2O during coal decoupling combustion in a circulating fluidized bed combustor using Aspen Plus. *Chem. Eng. Sci.* **2012**, *71*, 375–391, https://doi.org/10.1016/j.ces.2011.10.050.
43. Jang, D.-H.; Kim, H.-T.; Lee, C.; Kim, S.-H. Kinetic analysis of catalytic coal gasification process in fixed bed condition using Aspen Plus. *Int. J. Hydrogen Energy* **2013**, *38*, 6021–6026, https://doi.org/10.1016/j.ijhydene.2013.01.167.
44. Nikoo, M.B.; Mahinpey, N. Simulation of biomass gasification in fluidized bed reactor using ASPEN PLUS. *Biomass Bioenergy* **2008**, *32*, 1245–1254, https://doi.org/10.1016/j.biombioe.2008.02.020.
45. Damartzis, T.; Michailos, S.; Zabaniotou, A. Energetic assessment of a combined heat and power integrated biomass gasification–internal combustion engine system by using Aspen Plus®. *Fuel Process. Technol.* **2012**, *95*, 37–44, https://doi.org/10.1016/j.fuproc.2011.11.010.
46. Steag Energy Services Ebsilon®Professional 15.00. Available online: https://www.ebsilon.com/ (accessed on 22 September 2021).
47. Madejski, P.; Żymełka, P. *Introduction to Computer Calculations and Simulation of Energy Systems Operation in STEAG Eb-silon®Professional*; Wydawnictwa AGH: Kraków, Poland, 2020.
48. Soares, J.; Oliveira, A.; Valenzuela, L. A dynamic model for once-through direct steam generation in linear focus solar collectors. *Renew. Energy* **2021**, *163*, 246–261, https://doi.org/10.1016/j.renene.2020.08.127.
49. Yue, M.; Ma, G.; Shi, Y. Analysis of Gas Recirculation Influencing Factors of a Double Reheat 1000 MW Unit with the Reheat Steam Temperature under Control. *Energies* **2020**, *13*, 4253, https://doi.org/10.3390/en13164253.
50. Dahash, A.; Mieck, S.; Ochs, F.; Krautz, H.J. A comparative study of two simulation tools for the technical feasibility in terms of modeling district heating systems: An optimization case study. *Simul. Model. Pr. Theory* **2018**, *91*, 48–68, https://doi.org/10.1016/j.simpat.2018.11.008.
51. Mondal, S.K.; Uddin, M.F.; Majumder, S.; Pokhrel, J. HYSYS Simulation of Chemical Process Equipments. Available online: https://www.researchgate.net/publication/281608946_HYSYS_Simulation_of_Chemical_Process_Equipments (accessed on 22 September 2021).
52. Ziółkowski, P.; Kowalczyk, T.; Kornet, S.; Badur, J. On low-grade waste heat utilization from a supercritical steam power plant using an ORC-bottoming cycle coupled with two sources of heat. *Energy Convers. Manag.* **2017**, *146*, 158–173, https://doi.org/10.1016/j.enconman.2017.05.028.
53. Ziółkowski, P.; Kowalczyk, T.; Lemański, M.; Badur, J. On energy, exergy, and environmental aspects of a combined gas-steam cycle for heat and power generation undergoing a process of retrofitting by steam injection. *Energy Convers. Manag.* **2019**, *192*, 374–384, https://doi.org/10.1016/j.enconman.2019.04.033.
54. Werle, S.; Wilk, R.K. A review of methods for the thermal utilization of sewage sludge: The Polish perspective. *Renew. Energy* **2010**, *35*, 1914–1919, https://doi.org/10.1016/j.renene.2010.01.019.
55. Schweitzer, D.; Gredinger, A.; Schmid, M.; Waizmann, G.; Beirow, M.; Spörl, R.; Scheffknecht, G. Steam gasification of wood pellets, sewage sludge and manure: Gasification performance and concentration of impurities. *Biomass Bioenergy* **2018**, *111*, 308–319, https://doi.org/10.1016/j.biombioe.2017.02.002.
56. Akkache, S.; Hernández, A.-B.; Teixeira, G.; Gelix, F.; Roche, N.; Ferrasse, J.H. Co-gasification of wastewater sludge and different feedstock: Feasibility study. *Biomass Bioenergy* **2016**, *89*, 201–209, https://doi.org/10.1016/j.biombioe.2016.03.003.
57. Bonalumi D., Valenti G., Lillia S., Fosbol P.L., Thomsen K. A layout for the Carbon Capture with Aqueous Ammonia without Salt Precipitation. *Energy Procedia* **2016**, 86, 134–143, https://doi.org/10.1016/j.egypro.2016.01.014.
58. Campanari, S.; Chiesa, P.; Manzolini, G. CO2 capture from combined cycles integrated with Molten Carbonate Fuel Cells. *Int. J. Greenh. Gas Control* **2010**, *4*, 441–451, https://doi.org/10.1016/j.ijggc.2009.11.007.
59. Gou, C.; Cai, R.; Hong, H. An Advanced Oxy-Fuel Power Cycle with High Efficiency. *Proc. Inst. Mech. Eng. Part A J. Power Energy* **2006**, *220*, 315–325, https://doi.org/10.1243/09576509JPE215.

60. Liu, C.; Chen, G.; Sipöcz, N.; Assadi, M.; Bai, X. Characteristics of oxy-fuel combustion in gas turbines. *Appl. Energy* **2012**, *89*, 387–394, https://doi.org/10.1016/j.apenergy.2011.08.004.